Variational formulation of irreversible thermodynamics of surfaces and interfaces with grain-boundary triple-junction singularities under the capillary and electromigration forces in anisotropic two-dimensional space

Tarik Omer Ogurtani*
Department of Metallurgical and Materials Engineering, Middle East Technical University, 06531, Ankara, Turkey
(Received 18 September 2005; revised manuscript received 4 April 2006; published 13 June 2006)

A variational irreversible thermodynamic method for curved surfaces and interfaces in a two-dimensional (2D) continuum, having anisotropic specific surface Gibbs free energy, is developed by utilizing the more realistic monolayer model of Verschaffelt and Guggenheim for the description of interfaces and surfaces in connection with the global entropy production hypothesis. This approach considers not only the asymmetric disposition of the grain-boundary triple junction, but also its dynamical effects on the morphological evolution of surfaces. The governing Euler equation and the associated boundary conditions (the strong solution) are derived rigorously by the variational technique applied on the positive definite rate of global internal entropy production; the results are in excellent accord with those deduced by the first-principles theory of irreversible thermodynamics of curved surfaces with triple junctions as formulated previously by the author, using the basic postulate of the local internal entropy production in connection with the microfinite-element method in discrete 2D space. At the final stage, the whole problem is converted into a variational extremum problem in order to obtain the weak solution in a class of smooth functions (i.e., Hermite functions) having continuous derivatives $C_\infty(-\infty,+\infty)$ by transforming the displacement field into the particle-flux representation using the principle of conservation of particles, including the phase transition. As an application of the weak solution, which is converted into a compact matrix format in the normalized and scaled time and space domain, a set of computer simulation experiments is performed on symmetrically disposed bicrystal thin metallic films having fourfold anisotropic specific surface Gibbs free energy to demonstrate the breaching effects caused by grain-boundary grooving under the surface drift diffusion driven by the capillarity without electromigration forces.

DOI: 10.1103/PhysRevB.73.235408 PACS number(s): 68.35.Md, 68.35.Fx, 68.35.−p, 05.70.Np

I. INTRODUCTION

Capillary-driven morphological evolution of surfaces and interfaces in solids continues to be a challenging theoretical problem in materials science, especially under the action of applied force fields such as electromigration and thermomechanical stress systems. By drawing from elegant fundamental laws of physics, the field allows for the exciting possibility of making quantitative prediction about the behavior of a diverse range of real materials such as sapphire or ice. The importance of this subject in materials science applications derives from the fundamental role played by surfaces and heterophase boundaries in physical and chemical processes in solids, in stability of structures, and in properties of materials. Wetting, sintering, grain growth, grain-boundary grooving, growth of thin films, and stability of multilayers are all examples of capillary-driven shape and microstructural evolution. The special issue of surface morphological evolution has found renewed interest over the past decade with the advancement of nanotechnology. The evolution of a crystal surface close to a high-symmetry orientation (vicinal planes) has a stepped structure (terraces and breaching), and as a direct consequence of this the formation of cusps is observed in the Wulff construction of the surface specific Gibbs free energy below the roughening transition temperature. The evolution kinetics of such a surface is controlled by the surface drift diffusion as well as the evaporation and condensation processes occurring concurrently. This intricate behavior often combines with strong anisotropy (cusps) in the Wulff construction represented by a Dirac δ distribution function singularity in the surface stiffness, which is closely related to the instability of the surface morphological evolution, and the topography of the pattern formation.

In the early 1950s, this area was partially put into a solid quantitative framework by the classical work of Herring,[1] von Neumann,[2] and Mullins.[3] Their work relied strictly on equilibrium thermodynamics and the Gibbs[4] abstract description of interfaces and dividing surfaces. The earliest analytical study was Mullins[3] treatment of the grooving of a grain boundary (GB). Mullins ignored GB diffusion and considered the triple junction (TJ) to have an equilibrium capillarity configuration satisfying the Young[5] relationship. The boundary conditions at the TJ are continuity of the chemical potential, conservation of mass, and again the equilibrium capillarity configuration for the geometry. It has been well known for some time that GB grooves can develop facets owing to surface energy anisotropy. The presence of facets on the groove surfaces poses intricate modeling issues since Mullins' theory is inapplicable to anisotropic surfaces.

Non-boundary-tracking methods have been increasingly applied to simulate complex microstructural evolutions, including Monte Carlo, cellular automata, and phase field methods.[6] Kazaryan *et al.*[7] generalized the phase field approach by allowing for rigid-body rotation during sintering, and by further assuming that the TJ velocity can be determined from the steady-state requirement imposed at the GB. TJ motion is also investigated by Cahn *et al.*[8] utilizing long-time asymptotic analysis in which the requirement of uniform displacement is still incorporated. Averbuch *et al.*[9] utilized highly sophisticated numerical procedures in their

studies, but they still assumed that there is an equilibrium configuration at the TJ, and the TJ displacement velocity can be extrapolated from the projection of the normal velocities of the neighboring nodes in the direction of the intergranular GB.

The GB grooving at singular surfaces was extensively studied by Rabkin *et al.*[10] and Klinger *et al.*[11] by explicitly introducing faceted and rough regions, each with different isotropic surface energies. Recently, Zhang *et al.*[12] and Xin and Wong[13] prescribed an orientation-dependent surface stiffness instead of the surface free energy explicitly in their treatments. However, none of the above studies account for the grooving kinetics at the TJ, ruling out the possibility of a nonequilibrium groove profile, which was fully considered very recently by Ogurtani and Akyildiz[14] in connection with their extensive computer simulations under the capillary and electromigration forces. Actually, the results of the rigorous treatment of the nonequilibrium dynamics of the TJ by Oren and Ogurtani[15] appeared in the literature in connection with simulation studies of GB void interactions driven by electromigration and capillary forces in thin-film interconnects with bamboo structure having anisotropic diffusivity. In that study,[15] the asymmetric disposition of the adjacent grains (texture) is fully accounted for by the internal entropy production (IEP) due to the transversal virtual displacement of the TJ. The discrete micro-finite-element (DMFE) formulation of irreversible surface thermodynamics was also applied to the GB void interaction under the capillary and electromigration forces by Ogurtani and Oren,[16,17] and a formula resulted for the interconnect failure time that is in excellent agreement with the published experimental data on copper and aluminum thin-film interconnects having bamboo structures.

Most recently, Ramasubramaniam and Shenoy[18] made a very serious attempt to obtain a weak solution of the evolution kinetics of faceted GB grooves by using a variational approach and utilizing *ad hoc* thermokinetics arguments based on Herring's formula, which is very popular in surface science and continuum mechanics.[19] They produced, however, proper connections for the TJ displacement velocity, which is in complete accord with the result of Oren and Ogurtani,[15] but only for symmetrically disposed surface profiles that are initially flat and infinite in extent.

This paper focuses on the more transparent variational formulation of the irreversible thermodynamics of surfaces and interfaces to give a full coverage of the surface morphological evolution of arbitrary-shaped curved surfaces with corners and edges in both finite and infinite extent, utilizing not only the strong solutions but also the weak solutions of the problem. While doing that an asymmetrically disposed TJ singularity is also considered; this arises either due to the initial configuration of the system or because of the very intrinsic character of the anisotropic specific surface Gibbs free energy, which translates into the surface stiffness concept correlated with cusps in vicinal plane orientations in Wulff construction crystalline solids.[1] Even more severely asymmetric surface profiles occur at grain-boundary–triple-junction singularities during the morphological evolution under electromigration (EM) forces and/or under thermal strain field gradients generated by the steady-state heat flow through the interconnects. However, the strong solutions of these complications without the surface Gibbs free energy anisotropy have already been formulated by the present author in terms of the well-posed free-moving boundary-value problem. The results obtained by that approach were put into action during the extensive computer simulations of surfaces and interfaces by Ogurtani and co-workers.[14–16,20]

This paper is organized in the following manner. In Sec. II, the variational formalism of the irreversible thermodynamics of interfaces with GB-TJ singularities is elaborated rigorously by utilizing the positive definite global internal entropy production (GIEP) hypothesis. Here, the virtual displacements of the GB TJ as well as the ordinary points at the interfacial layer between two bulk phases are considered regardless of their states, whether they are solid/solid or solid/fluid composite systems. This unified approach results in a strong solution of the global nonequilibrium problem without referring to any thermokinetics relationships associated with the interfacial or bulk drift-diffusion phenomenon used in the context of the long-range mass-transfer processes. In Sec. III, the results obtained in Sec. II are combined with the law of conservation of particles to obtain a set of kinetic equations for ordinary and singular points (corners, edges, and GB-TJ singularities) along the solid surface layers, which relates the displacement velocity field to the particle-flux density representation. In the particle-flux formulation of GIEP, the asymmetrical disposition of the GB with respect to the surface layer is properly treated in addition to the anisotropy in surface specific Gibbs free energy. In Sec. IV, the weak solution of the extremum problem is formulated in the particle current density representation without putting any restriction on the asymmetrical disposition of bicrsytal samples. During the numerical treatment of the weak solution, we faced serious problems, which are solely associated with the naturally occurring discontinuities in the surface flux density and its gradient at the TJ singularity when the system is away from the equilibrium configuration. These problems are discussed thoroughly and remedies are proposed to smooth out those discontinuities by passing from the finite interfacial model to the Gibbs' continuum geometric representation using a simple mathematical technique familiar in calculus. In Sec. V, the numerical methods for the weak solution are elaborated, and the governing equation for the morphological evolution of grain-boundary thermal grooving is put into manageable matrix format. The tentative computer simulation experiments are executed on various asymmetric (texture) and symmetric GB configurations in nano-size ($\leqslant$100 nm) bicrsytal metallic interconnect lines to demonstrate the dynamics of thermal grooving, and the results obtained are compared with the available symmetric cases in the published literature.[18] Excellent agreements is found.

II. VARIATIONAL FORMULATION OF GLOBAL INTERNAL ENTROPY PRODUCTION

In this section, a variational irreversible thermodynamic method for the curved surfaces and interfaces in a two-dimensional (2D) continuum, having anisotropic specific surface Gibbs free energy, is developed by utilizing the more

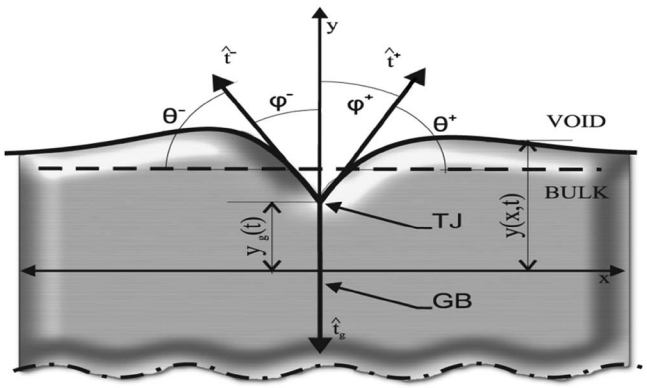

FIG. 1. Triple-junction macrostructure illustrates the asymmetrical evolution of the initially flat surface layer of a semi-infinite bulk matrix. $\{\hat{t}^+,\hat{t}^-,\hat{t}_g\}$ is the set of unit tangent vectors at the TJ, associated with the right- and left-side surface layers and grain-boundary-region layers.

realistic monolayer model of Verschaffelt[21] and Guggenheim[22] for the description of interfaces and surfaces, rather than the Gibbs abstract geometric model.[4]

The nonequilibrium treatment of the composite system considered here does not put any restriction on the state of the individual bulk phases whether they are solids or fluids, since it does not rely on any kinetic supplementary equations. Therefore, the findings of this section are also valid for the solid state phase transformation taking place between secondary phase particles and the matrix. The thermodynamic composite system consists of two bulk regions divided by a GB, and a realistic void phase (including the condensed state) separated by a singly connected curved interfacial layer (the generalized cylindrical surface in 3D). The GB and the void interfacial layers are both presumed to have finite and invariant thicknesses. The realistic void phase has well-defined thermodynamics properties, embedded in the bulk matrix, and attached to a straight and inflexible GB that lies along the y axis at the TJ, which is exposed to a lateral displacement constraint, as partly illustrated in Fig. 1. However, in the mathematical formulation of the problem presented in this section, these constraints on the GB are lifted completely to show the generality of our approach to this rather intricate and highly popular problem in the literature. The Gibbs specific surface free energy (GSFE) $g_g(\vartheta)$ associated with the GB is assumed to be anisotropic in this paper. Here ϑ is the angle between the tangent vector of the GB profile and the y axis. In Sec. III, the above-mentioned constraints again will be reimposed on the GB at the later stage of our treatment. This generalized approach not only contributes to the transparency of the treatment but also gives us an opportunity to recover the torque term associated with the anisotropic GB GSFE, which may have important contributions in the asymmetric cases.

In the present discussion, the subsystems are all completely open for the exchange of chemical species and energy, but the whole global system is closed. Each phase including the autonomous interfacial layers has a well-defined temperature and they are under complete thermal equilibrium. Therefore, all conceivable natural processes taking place in the global composite system are isothermal and irreversible.

The contribution due to the interfacial layer may be represented by the following anticlockwise contour integration in 2D space having a singularity at $x=0\pm\varepsilon$ and $y=0\pm\eta$ where the TJ is situated initially at the origin of a global laboratory reference system. Since there is a physical singularity at the GB TJ, this point will be treated as an external free end point (boundary), and the left- and right-hand sides of the surface layer with respect to the GB TJ are represented symbolically by the $\pm\vec{\varepsilon}(tj)$ finite position vector set. Similarly, the vector variation operators $\pm\delta\vec{\varepsilon}$ used in the following formulation denote the free virtual displacements of the left and right end points of the surface layer in the variational analysis, Hence, in the proposed analysis, the TJ is treated as a completely free-moving boundary point (free end point) having virtual displacements not only along the longitudinal (y axis) but also along the transverse direction (x axis). Then, one may write the following functional for the global Gibbs free energy of the system:

$$
\begin{aligned}
G\{y\} &= \oint_{+\vec{\varepsilon}\to-\vec{\varepsilon}} d\ell\; g_\sigma(\theta) + \int_{x=0,y=-h}^{\vec{\varepsilon}(TJ)} d\ell\; g_g(\vartheta) \\
&\quad + \int_{S_v} ds\; \breve{g}_v + \int_{S_b} ds\; \breve{g}_b \\
&= \oint_{+\vec{\varepsilon}\to-\vec{\varepsilon}} dx\; g_\sigma[\tan^{-1}(\tilde{y}_x)]\sqrt{1+\tilde{y}_x^2} + \int_{S_b} ds\; \breve{g}_b \\
&\quad + \int_{x=0,y(-h)}^{\vec{\varepsilon}(TJ)} dy\; g_g[\tan^{-1}(\tilde{x}_y)]\sqrt{1+\tilde{x}_y^2} + \int_{S_v} ds\; \breve{g}_v
\end{aligned}
\tag{1}
$$

where $\tilde{y}(x,t)$ and $\tilde{x}(y,t)$ are the surface and GB profile functions in the Cartesian coordinate system, $\vec{\varepsilon}(tj)$ denotes the temporal position of the GB-TJ singularity, $g_\sigma(\theta)$ is the orientation-dependent surface specific Gibbs free energy, and θ is the angle between the interface tangent vector and the x axis, as described in Fig. 1. The second term in the above equation represents the total Gibbs surface free energy of an initially straight but flexible GB having anisotropic GSFE. The symbol $\oint_{+\varepsilon\to-\varepsilon}$ indicates anticlockwise contour integration over the singly connected void surface layer between $+\vec{\varepsilon}$ and $-\vec{\varepsilon}$, where the temporal position of the TJ singularity is situated at the origin of the global Cartesian coordinate system for convenience. In Eq. (1) the GB-TJ singularity is treated as an external point, which constitutes a free-moving boundary in the formulation of the strong solution of the extremum problem. In general for closed-loop interfaces, $\tilde{y}(x,t)$ is a multivalued smooth surface profile function having piecewise continuous derivatives, and it should be represented in the parametric form during the contour integration. The third and fourth terms represent the global Gibbs free energies associated with the bulk phases separated by the interfacial layer. S_v and S_b are adjoining regions occupied, respectively, by the void and the embedding bulk phase, which are separated by the interfacial layer. The bulk solid regions that are separated by the GB may even be different

phases, and that does not change the results of the present formulation, since we have assumed an anisotropic surface Gibbs free energy and have put no restriction on the inhomogeneity of the bulk Gibbs free energy densities. Here $\breve{g}_v$ and $\breve{g}_b$ are the volumetric Gibbs free energy densities of the void and the bulk phases, respectively, and in general they may explicitly depend on the space and time. $g_\sigma(\theta)$ and $g_g(\vartheta)$ are specific surface Gibbs free energies of the interfacial layer and the GB, and they are related to the volumetric Gibbs free-energy densities by $g_\sigma=h_\sigma\breve{g}_\sigma$ and $g_g=h_g\breve{g}_g$, respectively. Here h_σ and h_g correspond to the thicknesses of the interfacial layer and the GB, respectively. In the geometric description (Gibbs model) of the interfaces and surfaces, where $(h_\sigma,h_g)\to 0$, these surface specific quantities still stay invariant, similar to the specific surface particle densities denoted by Γ_σ and Γ_g. The Gibbs free energy densities are generalized Gibbs free energies, and they are functions of not only the temperature and chemical composition but also the local stress tensor as well as the applied electric and magnetic field intensities.[20] Since we assumed that the system is under thermal equilibrium, the variation of the GIEP, δS_{int}, associated with the variation of the global Gibbs free-energy functional of the composite system due to the virtual displacement of the interfacial layer including the GB-TJ singularities may be given by the following expression:

$$\delta S_{IEP}\{\delta y,\pm\delta\vec{\varepsilon},\delta\vec{y}(0)\} = -\frac{1}{T}\left(\delta\oint_{+\delta\vec{\varepsilon}\to-\delta\vec{\varepsilon}} d\ell\; g_\sigma(\theta)+\delta\int_{y(-h)}^{\delta\vec{\varepsilon}(TJ)} d\ell\; g_g(\vartheta) +\oint_{+\vec{\varepsilon}\to-\vec{\varepsilon}}\delta\eta\, d\ell\;\Delta\breve{g}_{vb}\right)\geqslant 0 \tag{2}$$

where the $\pm\delta\vec{\varepsilon}$ and $\delta\vec{y}(0)$ vector displacement notations indicate that the end points of the above integral expression are free-moving points both along the x and y axes. In Eq. (2), $\Delta\breve{g}_{vb}=(\breve{g}_v-\breve{g}_b)$ is the volumetric Gibbs free-energy density of the transformation (GFEDOT) associated with the transformation of the bulk phase into a realistic void phase during the scooping motion[23] of the interface displacement. The connection between the GFEDOT and the specific Gibbs free energy of transformation Δg_{vb} between the parent phase and the void phase is $\Delta g_{vb}=h_\sigma\Delta\breve{g}_{vb}$. (Note that for evaporation of the bulk or growth of the void region, $\Delta g_{vb}<0$.) Here, we have also assumed implicitly that $\delta\Delta\breve{g}_{vb}\equiv 0$, which may be justified if one considers the fact that during the virtual displacement of the interfacial layer by the scooping action only the adjacent bulk regions are affected by the interfacial phase transformation. In the rigorous sense, this assumption automatically excludes the IEP associated with the bulk diffusion taking place for the redistribution of chemical species that are rejected by the interface displacement reaction in multicomponent systems (including athermal vacancies) during the phase transformation. Therefore, $\Delta\breve{g}_{vb}$ should be evaluated at the bulk regions that are just adjacent to the interface or beneath the surface layer.

Here the variations are considered not only with respect to the variation of the surface and GB profile functions at the ordinary points denoted by $\delta\tilde{y}(x,t)$ and $\delta\tilde{x}(y,t)$, but also includes the position of the TJ, which is assumed to be a completely free corner point (the refraction of the extremal), and may be described by the longitudinal $\delta(\pm\varepsilon_y)$ and transversal $\delta(\pm\varepsilon_x)$ displacement variations. Therefore, in the general treatment of the problem there are no constraints imposed on the lateral movements of the GB, which may separate two anisotropic grains in the bulk matrix having completely different physicochemical properties including the texture. Hence, one writes the following more explicit and exact expression in the Cartesian coordinate system by keeping in mind that the surface profile function is multivalued and piecewise continuous, and the integration is along the surface contour:

$$\delta S_{IEP}\{\delta y,\delta x,\delta(\pm\vec{\varepsilon}),\delta\vec{\varepsilon}(TJ)\} = -\frac{1}{\mathrm{T}}\lim_{|\varepsilon|\to 0}\left(\delta\oint_{+\delta\vec{\varepsilon}\to-\delta\vec{\varepsilon}} dx\; g_\sigma[\tan^{-1}(\tilde{y}_x)]\sqrt{1+\tilde{y}_x^2} +\delta\int_{y(-h)}^{\vec{\varepsilon}(TJ)} dy\; g_g[\tan^{-1}(\tilde{x}_y)]\sqrt{1+\tilde{x}_y^2}+\oint_{+\vec{\varepsilon}\to-\vec{\varepsilon}}\delta\eta\, d\ell\;\Delta\breve{g}_{vb}\right)\geqslant 0 \tag{3}$$

In above expression $\delta\eta=-(1+\tilde{y}_x^2)^{-1/2}\delta y$ is the virtual displacement of the interfacial layer along the surface normal and it is directed toward the bulk phase according to the convention adopted in our previous work.[20] In the second term of Eq. (3), we assumed that the GB specific Gibbs free energy is orientation dependent.

The variational problem described by Eq. (3) represents the general variation of a functional, which considers the arbitrary variations of the profile functions $\tilde{y}(x,t)$ and $\tilde{x}(y,t)$ and the arbitrary limits of integration (transversality conditions). This refraction extremal problem denoted explicitly by $\delta S_{IEP}\{\delta y,\delta x,\delta(\pm\vec{\varepsilon}),\delta\vec{y}(0)\}\equiv 0$ can have a weak solution if the Weiserstrass-Erdmann conditions are satisfied at corner points such as the TJ.[24] If we let the integrand in Eq. (3) denote by $F\Leftarrow g_\sigma[\tan^{-1}(\tilde{y}_x)]\sqrt{1+\tilde{y}_x^2}$, the following exact and general expression[25] can be written after first taking the variation of the integrand and then applying integration by parts, namely:

$$\begin{aligned}\lim_{|\varepsilon|\to 0}\delta\oint_{+\delta\vec{\varepsilon}\to-\delta\vec{\varepsilon}} dx\; g_\sigma[\tan^{-1}(y_x)]\sqrt{1+y_x^2} &= \lim_{|\varepsilon|\to 0}\delta\int_{+\delta\vec{\varepsilon}}^{-\delta\vec{\varepsilon}} dx\, F(x,y,y_x)\\ &= \lim_{|\varepsilon|\to 0}\Bigg[\int_{+\varepsilon}^{-\varepsilon} dx\left(F_y-\frac{d}{dx}F_{y_x}\right)\delta y+\left.F_{y_x}\right|_{x=-\varepsilon}\delta[y(-\varepsilon)]\\ &\quad+\left.(F-y_xF_{y_x})\right|_{x=-\varepsilon}\delta(-\varepsilon)-\left.F_{y_x}\right|_{x=+\varepsilon}\delta[y(+\varepsilon)]\\ &\quad-\left.(F-y_xF_{y_x})\right|_{x=+\varepsilon}\delta(+\varepsilon)\Bigg].\end{aligned} \tag{4}$$

The above relationship is written for a general type of integrand function denoted by $F(x,y,y_x)$. The second expression clearly and explicitly shows that the free variations of

the end points are along the lateral and the longitudinal directions as we proposed previously.

In the present case, the integrand has a simple form depending only on the derivative of the profile function denoted as y_x, which brings great simplification in the mathematical manipulations.

The Euler function $F_y-(d/dx)F_{y_x}$ may be immediately calculated using the fact that the ordinary derivative d/dx operator acts on F_{y_x} explicitly and implicitly, which gives the following results in two different formats using the definition of the integrand function as described above:

$$\left(F_y-\frac{d}{dx}F_{y_x}\right)=-\frac{d}{dx}F_{y_x}=-\frac{d}{dx}\{g'_\sigma\cos(\theta)+g_\sigma\sin\theta\}, \tag{5a}$$

$$\left(F_y-\frac{d}{dx}F_{y_x}\right)=-y_{xx}F_{y_xy_x}\equiv-\kappa\left[\frac{d^2g_\sigma}{d\theta^2}+g_\sigma\right]=-\kappa[g''_\sigma+g_\sigma]. \tag{5b}$$

The explicit expression Eq. (5a) is a very important form of the Euler equation and it will be used to obtain the weak solution of the smoothed-out particle-flux density later in Sec. IV. The implicit expression Eq. (5b) will be employed for the strong solution in Sec. III. The implicit expression is very popular in surface science for the description of the surface Gibbs free-energy anisotropy and in crystalline solids for the Wulff topographic representation of the vicinal surfaces. This function is also called Herring's surface chemical potential $\mu=-\kappa[g''_\sigma+g_\sigma]$ in the literature. In this formalism, $\tilde{g}_\sigma\equiv[g''_\sigma+g_\sigma]$ is called the surface stiffness and κ is used to denote the local curvature, which is assumed to be positive for a concave bulk surface. One may apply exactly the same variational procedure for the GB total specific Gibbs free energy represented by the second term in Eq. (3). Here, one can use the analogy and employ the quasisimilarity transformation $x\rightleftarrows y$ to get the connections very conveniently. However, we will not proceed along that line, but impose a constraint on the GB: inflexibility (but the GB still can move laterally as a rigid straight line), and only keep the term due to GB GSFE anisotropy, which does not drop out but rather yields the so-called torque term in Herring's celebrated work.[1]

If one combines Eqs. (3)–(5) and then divides both sides by the time increment δt, the following exact expression for the rate of global internal entropy production (RGIEP), which is a positive definite quantity, may be written after some rearrangements of the terms:

$$\frac{\delta S_{\rm int}}{\delta t}=-\frac{1}{T}\lim_{|\varepsilon|\to0}\Bigg[\oint_{+\varepsilon\to-\varepsilon}d\ell\{\kappa\tilde{g}_\sigma+\Delta\breve{g}_{vb}\}\frac{\delta\eta}{\delta t}+\Bigg((F-y_xF_{y_x})|_{x=-\varepsilon}-(F-y_xF_{y_x})|_{x=+\varepsilon}+\frac{\partial g_g(\vartheta)}{\partial\vartheta}\Bigg)\frac{\delta(\varepsilon)}{\delta t}+[(F_{y_x}|_{x=-\varepsilon}-F_{y_x}|_{x=+\varepsilon})+g_g(\vartheta)]\Bigg]\frac{\delta[\tilde{y}(0)]}{\delta t}\geqslant0. \tag{6}$$

In the arrangement of the first integral in Eq. (6), the following identities are employed: $\delta\eta=-(1+\tilde{y}_x^2)^{-1/2}\delta y$, $d\ell=(1+\tilde{y}_x^2)^{1/2}dx$, and $\kappa=\tilde{y}_{xx}(1+\tilde{y}_x^2)^{-3/2}$. That means that the positive direction of the surface normal is assumed to be toward the solid bulk phase, and the local curvature κ is taken to be positive for a concave solid surface (trough). The Weiserstrass-Erdmann[24] conditions state that the cofactors of $\delta(\varepsilon)$ and $\delta[\tilde{y}(0)]$ should be identically zero to have a weak solution in terms of a class of piecewise smooth continuous functions (continuous functions with derivatives having discontinuities at separate points, i.e., TJs).

Incidentally, in this paper we have given a tentative proof of these conditions during the formulation of the problem summarized by Eq. (4), if one recalls the definition of the weak solution. This shows the very close connection between the thermodynamic requirement of local equilibrium (isothermal reversible process) at the TJ and the Weiserstrass-Erdmann condition for the extremal (the stationary states in irreversible thermodynamics) having at least a weak piecewise smooth solution between the corner points. However, we are not interested in this extremal problem here; our main objective is to formulate the problem outside the isothermal reversible trajectory, namely, for the nonequilibrium case $\{\delta S_{int}/\delta t\}>0$. Since the system under consideration is in thermal equilibrium (isothermal natural processes), then $T\delta S_{int}/\delta t\geqslant0$ corresponds to the power dissipation function (Helmholtz function in German literature[26]), which has been extensively employed by Ogurtani and Seeger[27] in the treatment of the non-Stokesian viscosity associated with kinks (solitons) moving in an atmosphere of paraelastic mobile interstitials. Therefore, one may utilize this direct and physically more concrete approach for the extraction of the generalized forces (drag forces) and the conjugated velocities from Eq. (6), rather than using Onsager's postulate[28] on the decomposition of the entropy production into an arbitrary set of generalized forces and conjugated fluxes as mostly used in the literature. Then one may obtain the following relationships, which may be very important for interfaces separating two condensed phases, between those generalized drag forces and conjugated velocities using the linear connection between them, through the generalized phenomenological mobilities:

$$\frac{d\eta}{dt}=-\frac{\Re_{vb}}{kT}\Omega_b\{\kappa\tilde{g}_\sigma+\Delta\breve{g}_{vb}\}\quad\text{(interface velocity at ordinary point)}, \tag{7}$$

$$V_g^{long}|=-\frac{dy(0)}{dt}=\frac{\Re^{long}d_a}{kT}[(F_{y_x}|_{x=+\varepsilon}^{x=-\varepsilon})+g_g(\vartheta)]=\frac{\Re^{long}d_a}{kT}\{[(g_\sigma\sin\theta+g'_\sigma\cos\theta)|_{x=+\varepsilon}^{x=-\varepsilon}]+g_g[\vartheta]\}\quad\text{(longitudinal velocity)}, \tag{8}$$

and

$$V_g^{trans}|_{TJ} = \frac{d\varepsilon}{dt} = \frac{\Re^{trans} d_a}{kT}\left\{ (F - y_x F_{y_x})|_{x=-\varepsilon}^{x=+\varepsilon} - \frac{\partial g_g(\vartheta)}{\partial \vartheta} \right\}$$
$$= \frac{\Re^{trans} d_a}{kT}\left\{ (g_\sigma \cos\theta - g'_\sigma \sin\theta)|_{x=-\varepsilon}^{x=+\varepsilon} - \frac{\partial g_g(\vartheta)}{\partial \vartheta} \right\} \quad \text{(transverse velocity)} \tag{9}$$

where $\Re_{vb}$, $\Re^{long}$, and $\Re^{trans}$ are generalized mobility coefficients associated with the growth and the TJ longitudinal and transverse displacements. These generalized mobility coefficients have dimensions similar to the usual diffusion coefficients $[L^2/t]$. d_a is the mean interatomic distance, which converts force per length to force per particle units, and Ω_b is the mean atomic volume of the bulk phase. The positive directions of V_g^{long} and V_g^{trans} are toward the bulk region pointing along the GB line and the positive direction of the x axis $(-\varepsilon \to +\varepsilon)$. The angles θ^- and θ^+ used in the above relationships are acute angles with proper signs between the surface tangent vectors and the x axis as shown in Fig. 1. If one chooses a GB configuration similar to that of the present work, which is perpendicular to the initial flat surface, then one has simple connections between these angles and the corresponding dihedral angles $\phi^{\pm}$, namely, $\theta^+ = (\pi/2 - \phi^+)$, $\theta^- = (3\pi/2 + \phi^-)$. The general case where the GB is inclined to the surface can be easily deduced by simply replacing the angles $\theta^{\pm}$ in every formula cited in this paper by the dihedral angles denoted as $\phi^{\pm}$. Then to study the dynamical behavior of the GB-TJ singularity one obtains a set of mathematical formulas in term of the dihedral angles, which are invariant universal expressions and can be used for any arbitrary configuration of the system.

It should be mentioned here that each term appearing in the RGIEP is also a positive definite quantity, because the corresponding variations $\{\delta y, \delta x, \delta\vec{\varepsilon}\}$ are completely arbitrary. Therefore, we have obtained very important linear thermokinetics relationships [Eqs. (7)–(9)], which can also be applied to phase transformations in condensed states rather rigorously, without using any *ad hoc* kinetics arguments. The mathematical results obtained in this section may be directly used for computer simulations of the kinetics of the interface controlled phase transformation of a secondary phase particle in a bulk matrix, which is originally nucleated at the GB region. It may be very interesting to proceed further along the line proposed in this paper to study the case where the GB is completely flexible and can move under the action of the capillary forces. The contribution of a flexible GB to the total GIEP can be represented by the following explicit expression:

$$\frac{\delta S_{\text{int}}^{GB}}{\delta t} = -\frac{1}{T}\lim_{|\varepsilon|\to 0}\oint_{y(-h)\to y(0)} d\ell\{\kappa_g \tilde{g}_g\}\frac{\delta\xi}{\delta t} + [g_g \sin\vartheta + g'_g \cos\vartheta]\frac{\delta\varepsilon_x(TJ)}{\delta t} + [g_g \cos\vartheta - g'_g \sin\vartheta]\frac{\delta\varepsilon_y(TJ)}{\delta t} \geqslant 0 \tag{10}$$

where $\delta\xi/\delta t$ is the surface normal displacement velocity of the GB. The torque term for a straight rigid GB comes from the second term, and the contribution to the longitudinal displacement may be deduced from the third term by simply taking $\vartheta \to 0$ in Eq. (10).

III. THE STRONG SOLUTION FOR SOLID SURFACES

In this section, the GIEP hypothesis (positive definite) is elaborated further to suit the needs for the formulation of the morphological evolution of solid surfaces in terms of the particle-flux densities. To do that, some kinetics relationships, which were derived for the ordinary points and the GB-TJ singularities by employing the generalized law of conservation of particles that also considers the phase transition explicitly, have been taken into account. This formulation covers rigorously only those problems that are associated with a surface between a solid (bulk) and a vapor phase (void) including inviscid incompressible liquids. In the absence of particle (mass) source or sink, the surface displacement at the ordinary points (not at the singularities) along the surface normal is governed by a balance between the divergence of the atomic flux and the amount of mass accumulated or depleted at the interface. However, in this paper a more general case is considered, in which additional entropy source terms associated with the normal components of the incoming atomic flows from the bulk phase $\hat{J}_b$ and the realistic void region $\hat{J}_v$ due to condensation or evaporation processes are included. These two terms are additive because of the adopted positive directions of flows, $\hat{J}_{vb} = \hat{J}_v + \hat{J}_b$. Hence the following kinetic expression applies for the conservation of atomic species during the virtual displacement of the ordinary points on the curved surface layer, having no variation in thickness due to stretching:

$$[(c_b - c_v) - h_\sigma \kappa c_\sigma]\frac{d\eta}{dt} = \frac{\partial J_\sigma}{\partial \ell} - \hat{J}_{bv}. \tag{11}$$

c_b, c_v, and c_σ are the atomic volumetric concentrations associated with bulk, void, and surface phases, respectively. As a special case of the above expression, if one assumes that a realistic void is a polyatomic dilute gas, in which $c_v \cong 0$, uses the argument of Guggenheim[22] related to the very existence of the concept of the interfacial layers $\kappa h_\sigma \cong 0$, and the expression $\Omega_b = c_b^{-1}$, the following results are obtained (excluding the TJ singularity):

$$\frac{d\eta}{dt} = \hat{n}\cdot\frac{\partial\vec{r}}{\partial t} = \Omega_b\left(\frac{\partial J_\sigma}{\partial \ell} - \hat{J}_{vb}\right) \quad \text{and} \quad \frac{\partial y(x,t)}{\partial t} = -\Omega_b\left(\frac{\partial J_\sigma}{\partial x} - \hat{J}_{vb}^y\right), \tag{12}$$

where $\hat{n}$ and $\vec{r}$ are the surface normal (directed toward the bulk phase) and the position vectors, respectively. $J_{vb}^y = \hat{J}_{vb}\sec\theta$ is the y component of the net incoming flux into the surface layer (2D surface phase) from the adjacent bulk phase and the realistic void region. Equation (12) may also be applied for an interfacial layer between a solid substrate and an inviscid incompressible liquid or even for an amor-

phous solid having high fluidity at high temperatures. Because these substances can easily allow and transmit mass by convection currents or shear strain relaxation mechanisms for the local shape changes caused by the virtual displacement of the surface layers of the underlying crystalline solids, which are assumed to have high rigidity. These shape changes are solely due to nonvanishing divergence (mass accumulation) of the particle current density driven by the interfacial drift diffusion. The drift-diffusion-induced shape changes are very slow movements (creeping motion) compared to the fast convection currents in the hypothetical low viscosity fluids.

Equation (12) describes the law of conservation of mass in terms of particle flux for the ordinary points, where the flux is presumed to be describable by smooth functions having derivatives that may have discontinuities at singularities. Therefore, the above equation cannot be applied to the GB-TJ singularities, where even the surface current density shows a Dirac-type singularity because the local curvature goes to infinity. The application of the same conservation law to the free-moving GB TJ (without stretching but only extending[4]) gives the following relationship if one takes properly into account the mass gained or lost by the GB layer (the phase transition) during longitudinal displacement:

$$\Gamma_g V_g^{long} \equiv J^+ - J^- - J_g, \tag{13}$$

where, according to our adopted convention, J^- and J_g are incoming fluxes from the negative side of the void surface layer and the GB region, and J^+ is the void surface flux coming out from the TJ by assuming that the positive direction of the surface particle flux is counterclockwise (from left to right for the flat surfaces). $\Gamma_g \equiv \Omega_g^{-1} h_g$ is the grain-boundary specific surface particle density, and is an invariant intensive quantity. $\Gamma_g V_g^{long}$ is the rate of particle loss or gain by the GB layer during the displacement of the TJ. Ω_g and Ω_σ are the mean atomic volumes in the GB region and in the solid surface layer, respectively, and roughly equal to their counterparts for the bulk solid phase. The positive direction of V_g^{long} is assumed to be toward the GB region. Actually, this phase transformation is one of the main sources for the local IEP at the GB-TJ singularity as demonstrated in our earlier work,[17] and furnishes the generalized force for the establishment of the partial equilibrium at the GB-TJ singularity along the longitudinal direction. The second main source for the local IEP is the nonequilibrium lateral displacement of the GB-TJ singularity, which furnishes the required generalized driving force for the lateral surface drift diffusion or for the lateral displacement of the GB-TJ singularity, depending upon whether the GB is subjected to the lateral constraint or not, respectively. The latter case is closely associated with the GB sliding, which may be formulated in the future.

To obtain an analytical relationship between the surface drift-diffusion flux and the intrinsic thermophysical intensive properties of the system, the generalized conservation expression for the ordinary points, Eq. (12), may be substituted into Eq. (6) together with our previous results summarized in Eqs. (7)–(9). If one applies the integration by parts to the first integral expression in Eq. (6) that is initially modified by the kinetic expression in Eq. (11) then the following relationship arises:

$$\begin{aligned}\frac{\delta S}{\delta t} = \frac{1}{T} \lim_{|\varepsilon|\to 0} & -\langle \Omega_b \{\kappa \tilde{g}_\sigma + \Delta \breve{g}_{vb}\} J_\sigma|_{+\varepsilon}^{-\varepsilon} \rangle \\ & + \Omega_b \int_{-\infty\to-\varepsilon}^{+\varepsilon\to+\infty} d\ell\, J_\sigma \frac{\partial}{\partial \ell}\{\kappa \tilde{g}_\sigma + \Delta \breve{g}_{vb}\} \\ & + \Omega_b \int_{-\infty\to-\varepsilon}^{+\varepsilon\to+\infty} d\ell\, \hat{J}_{vb}\{\kappa \tilde{g}_\sigma + \Delta \breve{g}_{vb}\} - \Bigg\{ (g_\sigma \cos\theta \\ & - g'_\sigma \sin\theta)|_{x=+\varepsilon}^{x=-\varepsilon} + \frac{\partial g_g(\vartheta)}{\partial \vartheta} \Bigg\} \Gamma_\sigma^{-1} J^{trans} + \{([g_\sigma \sin\theta \\ & + g'_\sigma \cos\theta)|_{x=+\varepsilon}^{x=-\varepsilon}] + g_g(\vartheta)\} V_g^{long} \geqslant 0. \end{aligned} \tag{14}$$

Here, one has $(\kappa \tilde{g}_\sigma + \Delta \breve{g}_{vb}) J_\sigma|_{-\infty\to-\varepsilon}^{+\varepsilon\to+\infty} \Rightarrow (\kappa \tilde{g}_\sigma + \Delta \breve{g}_{vb}) J_\sigma|_{+\varepsilon}^{-\varepsilon}$ since $J_\sigma \to 0$ and $\partial J_\sigma / \partial x \to 0$ at infinity because of our assumption of the validity of the natural boundary conditions for the initial flat surface layer. The first term in the RGIEP, which also appears in our discrete micro-finite-element method formulation,[16,20] written intentionally between angular brackets to emphasize its importance. This term and its consequences are very important in general, excluding the special case where the system has a complete reflection symmetry with respect to the GB orientation (bicrystal with twin orientation), and in addition there is no electrostatic and/or elastostatic force (no external force field). This term has been missed without showing sufficient mathematical or physical justification by Ramasubramaniam and Shenoy[18] in their formulation of the weak solution of the extremum problem especially in the derivation of their basic relationship, Eq. (13) in Ref. 18, in contrast to the presentation of Eq. (A.5) in Ref. 18, where reflection symmetry is invoked verbally and properly.

In the above expression, the RGIEP is converted partially into the particle-flux representation $J_\sigma^{trans}(0) = \Gamma_\sigma V_g^{trans}$ by first assuming the lateral motion of the TJ is restricted and then postulating that the thermodynamic generalized force is diverted to act on the surface particle flux as a driving force to establish the required lateral equilibrium at the GB TJ. Since by hypothesis the RGIEP is a positive definite quantity for any arbitrary variations in the particle fluxes $\{J_\sigma, J_{vb}\}$ and in the displacements of the GB TJ, then all terms in the above expressions, including the integrands under the integration operations, are positive quantities, and can be decomposed into generalized forces and conjugated fluxes accordingly to Onsager's hypothesis,[29] which gives

$$J_\sigma = \frac{M_\sigma}{kT} \Omega \frac{\partial}{\partial \ell}\{\kappa \tilde{g}_\sigma + \Delta \breve{g}_{vb}\} \quad \text{(surface drift-diffusion flux)}, \tag{15}$$

$$\hat{J}_{vb} = \Omega_b \frac{M_{vb}}{kT}\{\kappa \tilde{g}_\sigma + \Delta \breve{g}_{vb}\} \quad \text{(evaporation and condensation flux)}, \tag{16}$$

$$J_{\sigma}^{trans}\big| = \frac{\Re^{trans} d_a \Gamma_g}{kT}\Bigg((g_{\sigma}^{+}\cos\theta^{+} - g_{\sigma}^{\prime +}\sin\theta^{+}) - \frac{\partial g_g(\vartheta)}{\partial \vartheta} - (g_{\sigma}^{-}\cos\theta^{-} - g_{\sigma}^{\prime -}\sin\theta^{-})\Bigg) \quad \text{(transverse flux)}, \tag{17}$$

and

$$V_{g}^{long}\big| = \frac{\Re^{long} d_a}{kT}[-(g_{\sigma}^{+}\sin\theta^{+} + g_{\sigma}^{\prime +}\cos\theta^{+}) + (g_{\sigma}^{-}\sin\theta^{-} + g_{\sigma}^{\prime -}\cos\theta^{-}) + g_g(\vartheta)] \quad \text{(longitudinal velocity)}. \tag{18}$$

Although the above relationships are necessary and sufficient to build up the strong solution of the boundary value problem if one combines them with the generalized mass conservation laws [e.g., Eq. (12) for the ordinary points and Eq. (13) for the GB-TJ singularities], the following one extra inequality also arises rigorously:

$$-\frac{1}{T}\langle \Omega_b\{\kappa\tilde{g}_{\sigma} + \breve{g}_g\} J_{\sigma}\big|_{+\varepsilon}^{-\varepsilon}\rangle \geqslant 0. \tag{19}$$

This connection in the case of the strong solution is embedded in the boundary conditions through the kinetics relationships Eqs. (12) and (13), but it will be fully recovered in the weak solution of the extremum problem treated in this paper. The importance of this IEP source may be more appreciated in the case of corners and edges of the surface layer, where the current density $J_{\sigma}^{c+} = J_{\sigma}^{c-} \equiv J_{\sigma}^{corn}$ and the bulk Gibbs free energies of the individual phases, $\Delta\breve{g}_{vb}^{+} = \Delta\breve{g}_{vb}^{-}$, are strictly continuous functions of space. Then one may write the following expression for the current density at the corners or edges using the Onsager linear connection in irreversible thermodynamics between the generalized forces and the conjugated fluxes (by neglecting the cross terms):

$$J_{\sigma}^{TJ} = \frac{M_{\sigma}^{\pm}}{kT}\Gamma_{\sigma}\Omega_b\{\kappa^{+}\tilde{g}_{\sigma}^{+} - \kappa^{-}\tilde{g}_{\sigma}^{-}\} = \frac{M_{\sigma}^{\pm}}{kT}\Gamma_{\sigma}(\mu_{\sigma}^{+} - \mu_{\sigma}^{-}), \tag{20}$$

where $M_{\sigma}^{\pm}$ denotes the generalized mobility associated with discontinuous change in the chemical potential due to the capillarity across the GB-TJ singularity or at the sharp corners and edges of the surface profile function. This mobility has no apparent physicochemical connection with the surface diffusion mobility denoted by M_{σ} at the GB-TJ singularity. This relationship clearly and irrevocably shows that the nonvanishing particle current flux takes place at the corners and edges, where either the curvatures and/or the surface stiffness (due to the abrupt change in slope) may show some discontinuities. This nonvanishing particle current flux is proportional to the difference in the surface chemical potentials as defined in the sense of Herring's relationship. To our knowledge, this is the first reported analytical expression in the present context obtained rigorously by the irreversible thermodynamics of surfaces. This relationship also shows as expected *a priori* that not only the gradient of the surface chemical potential but also the difference acts as a driving force for the surface particle flow. The same contribution also appeared in the formulation of GIEP in our previous publications [see Eq. (38) in Ref. 17 and Eq. (1) in Ref. 20] without interpretation.

A careful examination of this section shows that the thermodynamics relationships cited by Eqs. (15)–(18) in conjunction with Eqs. (12) and (13), obtained previously by the direct application of the law of conservation of particles (i.e., mass) into two completely distinct cases having different contexts (ordinary and singular points), constitute the basis for the strong solution in terms of a moving free boundary value problem. The governing partial differential equation describing the kinetics of the surface morphological evolution in terms of the normal displacement velocity can be obtained by substituting Eqs. (15) and (16) into Eq. (12), which gives

$$V_{\sigma} = \hat{n}\cdot\frac{\partial \vec{r}_{\sigma}}{\partial t} = \Omega_b^2\frac{\partial}{\partial \ell}\Bigg(\frac{D_{\sigma}\Gamma_{\sigma}}{kT}\Bigg\{\frac{\partial}{\partial \ell}[\{\kappa\tilde{g}_{\sigma} + \Delta\breve{g}_{vb}\} + e|Z|\varphi/\Omega_b]\Bigg\}\Bigg) - \Omega_b^2\frac{M_{vb}}{kT}\{\kappa\tilde{g}_{\sigma} + \Delta\breve{g}_{vb}\}. \tag{21}$$

Here, the electromigration force, which is used in our computer simulations, is also added as an external force on the surface drift diffusion. In the above expression, $e|Z|$ is the effective electromigration charge and φ is the electrostatic potential. $M_{\sigma} = D_{\sigma}\Gamma_{\sigma}$ and $D_{\sigma}(\theta,\varphi)$ are the generalized mobility and the surface drift-diffusion coefficients, which may be anisotropic and depend on the surface orientation θ and the tilt angle ϕ of the principal axis of the diffusion dyadic with respect to some chosen global coordinate system attached to the specimen.

The set of the necessary and sufficient boundary conditions at the GB-TJ singularity can be easily written in terms of the incoming and outgoing surface fluxes $\{J_{\sigma}^{\pm}\}$ plus the displacement velocity V_g^{long} by using Eq. (13) and Eqs. (17) and (18). While doing that one should remember that there is a complete freedom in the choice of the incoming and outgoing surface fluxes to the GB-TJ singularity as long as they satisfy the law of conservation of particles presented by Eq. (13). In our earlier papers,[17] we have composed them symmetrically with respect to the TJ by artificially dividing the specific Gibbs free energy and the incoming GB flux into two parts. In this paper, we take a different approach and assign the transversal flux to the incoming flux; hence one may write

$$J_{\sigma}^{-} = J_{\sigma}^{trans} + J_{\sigma}^{TJ} = \frac{\Re^{trans} d_a \Gamma_g}{kT}\Bigg((g_{\sigma}^{+}\cos\theta^{+} - g_{\sigma}^{\prime +}\sin\theta^{+}) - (g_{\sigma}^{-}\cos\theta^{-} - g_{\sigma}^{\prime -}\sin\theta^{-}) - \frac{\partial g_g(\vartheta)}{\partial \vartheta}\Bigg) + J_{\sigma}^{TJ} \tag{22}$$

and

$$J^{+} \equiv J_g + J^{-} + \Gamma_g V_g^{long} = J_g + J_\sigma^{TJ} + \frac{\Re^{trans} d_a \Gamma_g}{kT}\Bigg[(g_\sigma^{+}\cos\theta^{+} - g_\sigma'^{+}\sin\theta^{+}) - \frac{\partial g_g(\vartheta)}{\partial\vartheta} - (g_\sigma^{-}\cos\theta^{-} - g_\sigma'^{-}\sin\theta^{-})\Bigg] + \frac{\Re^{long} d_a \Gamma_g}{kT}[-(g_\sigma^{+}\sin\theta^{+} + g_\sigma'^{+}\cos\theta^{+}) + (g_\sigma^{-}\sin\theta^{-} + g_\sigma'^{-}\cos\theta^{-}) + g_g]. \tag{23}$$

The above two expressions plus the longitudinal GB-TJ displacement velocity, Eq. (18), constitute necessary and sufficient boundary conditions for the governing equation [Eq. (21)] presented above to form a well-posed boundary value problem for the singly connected void surfaces or a solid surface having infinite extent with natural boundary conditions. These results are identical to those obtained by the DMFE formulation with[30] and without[16] anisotropy in the surface Gibbs free energies.

A careful examination of Eqs. (7) and (8) indicates that in the case of thermodynamic equilibrium (reversible processes), which is represented by $\delta S_{IEP}=0$, the following connections concerning the equilibrium configuration of the TJ may be deduced: $V_g^{long}=0$ and $V_g^{trans}=0$. These two equalities may be multiplied by the unit vectors $\hat{j}$ and $\hat{\imath}$ in the Cartesian coordinate system, respectively. The summation of the results can be put into the following vectorial format after some legal manipulations:

$$\vec{F}_{TJ} = \Bigg\{ g_g \hat{t}_g + g_\sigma^{+}\hat{t}^{+} + g_\sigma^{-}\hat{t}^{-} + \Bigg(\frac{\partial g_\sigma^{+}}{\partial\theta^{+}}\hat{k}\times\hat{t}^{+} + \frac{\partial g_\sigma^{-}}{\partial\theta^{-}}\hat{k}\times\hat{t}^{-} + \frac{\partial g_g}{\partial\vartheta}\hat{k}\times\hat{t}_g^{+}\Bigg)\Bigg\} = 0 \tag{24}$$

where $\hat{t}_g$, $\hat{t}^{+}$, and $\hat{t}^{-}$ are the unit vectors associated with the GB and right- and left-hand interfacial segments, respectively, and pointed away from the TJ. $\hat{k}=t^{+}\times t^{-}$ is a unit vector normal to the cut surface presented in Fig. 1. This relationship is also obtained by the author utilizing the generalized concept of the affinity of the interfacial displacement reactions in anisotropic media, in the formulation of the irreversible thermodynamics of surfaces using the micro-discrete-element method,[30] where the chemical potentials of the individual species are orientation dependent.

The above vector representation is exactly identical in mathematical form to $\partial g_i/\partial\hat{t}_i=(\partial g_i/\partial\theta_i)\hat{k}\times\hat{t}_i$, which is mostly used in the literature,[31] but it has a completely different context compared to the one obtained by Herring[1] relying on the Gibbs abstract geometric construction of a dividing surface, where the notion of line tension is mixed up with the immeasurable or ill-defined excess Helmholtz free-energy difference.

IV. WEAK SOLUTION OF THE EXTREMUM PROBLEM

Before making any further advancement, we should show that the awkward situation observed in the strong solution related to the Dirac δ function singularity in the gradient of the current density may be relaxed by using the following very plausible relationship denoted by Eq. (25). This relationship is definitely valid in the discrete representation, since the GB TJ is no longer a geometric point but is a 2D region in the Guggenheim model[22] for surfaces and interfaces. To connect the discrete and continuum representations one may introduce the following popular procedure in the calculus by using Eqs. (13) and (18):

$$\left.\frac{\partial J_\sigma}{\partial x}\right|_{x=0} \overset{\text{def}}{\cong} \lim_{h_g\to 0}\left(\frac{J_\sigma|_{-\varepsilon}^{+\varepsilon}}{h_g}\right) = \Omega_b^{-1} V_g^{long} = \Omega_b^{-1}\frac{\Re^{long}}{kT} d_a[(\,(g_\sigma\sin\theta + g_\sigma'\cos\theta)|_{x=+\varepsilon}^{x=-\varepsilon}) + g_g]. \tag{25}$$

This relationship may justify the *ad hoc* usage of the particle-flux gradient at the TJ by assuming that it is finite and continuous there for the formulation of the weak solution of the extremal problem. The following simple relationship, which may be obtained from Eqs. (23) and (25), is very important for the later formulation of the weak solution, and also shows the direct mathematical connection at the limit between the finite interface model of Guggenheim and the Gibbs geometric continuum model of interfaces at the GB-TJ singularity:

$$J^{+} \equiv J_g + J^{-} + \Gamma_g V_g^{long} \Rightarrow J_g + J^{-} + h_g \left.\frac{\partial J}{\partial x}\right|_{x=0}. \tag{26}$$

In the development of the weak solution of the extremum problem, there is only one criterion that should be satisfied in the choice of functional, namely, its strong solution should be consistent with the strong solution of the problem by the RGIEP formalism, with some legitimate smoothing-out procedures applied to the boundary conditions. Now, let us write the following variational functional over the range of admissible particle fluxes using the standard technique.[19,32]

$$\Xi\{J_\sigma,\hat{J}_{vb}\} \cong -T\frac{\delta S_{\text{int}}\{J_\sigma,\hat{J}_{vb}\}}{\delta t} + \int_{-\infty}^{+\infty} d\ell \frac{{J_\sigma}^2}{2\hat{M}_\sigma} + \int_{-\infty}^{+\infty} d\ell \frac{{\hat{J}_{vb}}^2}{2\hat{M}_{vb}} + \frac{\Gamma_\sigma}{2d_a\hat{M}^{long}}\left(\Omega\frac{\partial J_\sigma}{\partial x}\right)_{x=0}^2 + \frac{\Gamma_\sigma^{-2}J_\sigma^2(0)}{2d_a\hat{M}^{trans}} + \frac{J_\sigma^2(0)}{2\hat{M}^{\pm}}, \tag{27}$$

where the last term, which is missing in the above-cited reference [see Eq. (13) in Ref. 17], is added to the newly defined extremum problem to complete the rigorous treatment of the problem. This contribution associated with the IEP denoted by $-(1/T)\langle\Omega_b\{\kappa\tilde{g}_\sigma+\breve{g}_g\}J_\sigma|_{+\varepsilon}^{-\varepsilon}\rangle \geqslant 0$, which arises in the integration of Euler's integral in Eq. (14) by parts. As stated above, this is closely related to the corners and edges of the surface profile function like the GB TJ, where some finite discontinuities may occur in the curvature and/or in the specific Gibbs surface free energies. $\hat{M}_\sigma=\Re_\sigma\Gamma_\sigma/kT$, $\hat{M}^{trans}=\Re^{trans}\Gamma_\sigma/kT$, $\hat{M}^{long}=\Re^{long}\Gamma_\sigma/kT$, $\hat{M}_{vb}=\Re_{vb}\Gamma_\sigma/kT$, and $\hat{M}^{\pm}$ are the generalized mobility coefficients, which contain $1/kT$

terms as cofactors, implicitly.[17] During the normalization of the generalized mobilities with respect to the surface diffusion mobility, one may realized that $\hat{M}_{vb}$ and $M^{\pm}$ have two and one order deficiencies compared to other mobilities, namely, $\bar{M}_{vb}=\hat{M}_{vb}\ell_0^2/\hat{M}_{\sigma}$ and $\bar{M}^{\pm}=\hat{M}\ell_0/\hat{M}_{\sigma}$, where ℓ_0 is the arbitrary scaling length. Hence, one may deduce the following explicit extremum expression for the newly defined functional denoted as Eq. (27) by substituting Eqs. (13) and (17):

$$\delta\Xi\{\delta J_{\sigma},\delta J_{vb}\}\cong\delta\Bigg\{J_{\sigma}(0)\Omega_b(\kappa\tilde{g}_{\sigma}+\Delta\breve{g}_{vb})\big|_{+\varepsilon}^{-\varepsilon}-\Omega_b\int_{-\infty\to-\varepsilon}^{+\varepsilon\to+\infty}d\ell\,J_{\sigma}\frac{\partial}{\partial\ell}(\kappa\tilde{g}_{\sigma}+\Delta\breve{g}_{vb})-\Omega_b\int_{-\infty\to-\varepsilon}^{+\varepsilon\to+\infty}d\ell\,\hat{J}_{vb}(\kappa\tilde{g}_{\sigma}+\Delta\breve{g}_{vb})+\{(g_{\sigma}\cos\theta$$
$$-g'_{\sigma}\sin\theta)\big|_{x=+\varepsilon}^{x=-\varepsilon}+g'_{g}\}\Gamma_{\sigma}^{-1}J_{\sigma}(0)-\{[(g_{\sigma}\sin\theta+g'_{\sigma}\cos\theta)\big|_{x=+\varepsilon}^{x=-\varepsilon}]+g_g\}\Omega\left.\frac{\partial J_{\sigma}}{\partial x}\right|_{x=0}+\frac{\Gamma_{\sigma}^{-2}J_{\sigma}^2(0)}{2d_a\hat{M}^{trans}}+\int_{-\infty}^{+\infty}d\ell\,\Gamma_{\sigma}^{-1}\frac{J_{\sigma}{}^2}{2\hat{M}_{\sigma}}$$
$$+\int_{-\infty}^{+\infty}d\ell\frac{\hat{J}_{vb}^2}{2\hat{M}_{vb}}+\frac{\Gamma_{\sigma}}{2d_a\hat{M}^{long}}\left[\left(\Omega\frac{\partial J_{\sigma}}{\partial x}\right)\right]_{x=0}^2+\frac{J_{\sigma}^2(0)}{2\hat{M}^{\pm}}\Bigg\}=0. \tag{28}$$

The variational treatment of the above expression, with respect to the surface current density, δJ_{σ}, and the incoming bulk current flux, $\delta\hat{J}_{vb}$, shows that the particle-flux densities satisfying the extremum conditions of the functional $\delta\Xi\{\delta J_{\sigma},\delta J_{vb}\}=0$ yield the following relationships:

$$J_{\sigma}=\frac{\Re_{\sigma}\Gamma_{\mathrm{b}}}{kT}\Omega_{\mathrm{b}}\frac{\partial}{\partial\ell}\{\kappa\tilde{g}_{\sigma}+\Delta\breve{g}_{vb}\}$$
(surface flux at ordinary points), (29)

$$\left.\frac{\partial J_{\sigma}}{\partial x}\right|_{x=0}\cong\hat{M}_{long}\frac{d_a}{h_{\sigma}}\{[(g_{\sigma}\sin\theta+g'_{\sigma}\cos\theta)\big|_{x=+\varepsilon}^{x=-\varepsilon}]+g_g\}, \tag{30}$$

$$J_{\sigma}\big|_{x=0}=\hat{M}_{trans}d_a\{(g_{\sigma}\cos\theta-g'_{\sigma}\sin\theta)_{x=-\varepsilon}^{x=+\varepsilon}-g'_g\}\big|, \tag{31}$$

$$\hat{J}_{vb}=\hat{M}_{vb}\Omega_b\{\kappa\tilde{g}_{\sigma}+\Delta\breve{g}_{vb}\}$$
(evaporation and condensation flux), (32)

and

$$J_{\sigma}^{TJ}(0)=M_{\sigma}^{\pm}\Omega_b(\kappa\tilde{g}_{\sigma}+\Delta\breve{g}_{vb})\big|_{-\varepsilon}^{+\varepsilon}$$
(surface flux at corner and edges). (33)

A close inspection of the above set of equations shows that they are simply smoothed-out versions of the counterpart strong solution of the problem in the geometric continuum representation. Therefore, as expected *a priori*, the weak solution of the GB grooving may lose some fine morphological details especially at the groove tip in the case of strong surface stiffness anisotropy, and that should be checked by computer simulations and compared with the strong solution.

To obtain the weak solution by the modified Ritz method in the particle current representation, another strategy is adopted, which is also employed by Ramasubramanian and Shenoy[18] in their paper for the symmetrical case. That is, the derivative form of the Euler equation presented in Eq. (5) is used in Eq. (14) during the integration by parts. Hence, one may write

$$\delta\Xi\{\delta J_{\sigma},\delta J_{vb}\}\cong\delta\Bigg\{\Omega_b\int_{-\infty}^{+\infty}d\ell\left\{\Delta\breve{g}_{vb}+\frac{d}{dx}\{g'_{\sigma}\cos(\theta)+g_{\sigma}\sin\theta\}\right\}\left(\frac{\partial J_{\sigma}}{\partial\ell}\right)-\Omega_b\int_{-\infty}^{+\infty}d\ell\{\kappa\tilde{g}_{\sigma}+\Delta\breve{g}_{vb}\}\hat{J}_{vb}+\Bigg|\{(g_{\sigma}\cos\theta$$
$$-g'_{\sigma}\sin\theta)_{x=+\varepsilon}^{x=-\varepsilon}+g'_g\}\Gamma_{\sigma}^{-1}J_{\sigma}(0)\quad+\frac{\Gamma_{\sigma}^{-2}J_{\sigma}^2(0)}{2\hat{M}^{trans}}-\{[(g_{\sigma}\sin\theta+g'_{\sigma}\cos\theta)\big|_{x=+\varepsilon}^{x=-\varepsilon}]+g_g\}\left(\Omega_b\frac{\partial J_{\sigma}}{\partial x}\right)_{x=0}+\frac{J_{\sigma}^2(0)}{2\hat{M}^{\pm}}$$
$$+\int_{-\infty}^{+\infty}d\ell\,\Gamma_{\sigma}^{-1}\frac{J_{\sigma}{}^2}{2\hat{M}_{\sigma}}+\int_{-\infty}^{+\infty}d\ell\frac{\hat{J}_{vb}{}^2}{2\hat{M}_{vb}}+\frac{\Gamma_{\sigma}}{2d_a\hat{M}^{long}}\left(\frac{\Omega_b\partial J_{\sigma}}{\partial x}\right)_{x=0}^2\Bigg\}=0. \tag{34}$$

The application of integration by parts on the first integral expression by assuming that the current densities $\{J_{\sigma},J_{vb}\}$ and their derivatives go to zero at $x\to\pm\infty$ yields the following relationship after some trivial cancellations:

$$\delta\Xi\{J_\sigma,J_{vb}\} \cong \delta\Bigg[-\Omega_b\int_{-\infty}^{+\infty} dx\{g'_\sigma\cos(\theta)+g_\sigma\sin\theta\}\frac{\partial^2 J_\sigma}{\partial x^2}+\Omega_b\int_{-\infty}^{+\infty} dx\{\Delta\breve{g}_{vb}\}\left(\frac{\partial J_\sigma}{\partial x}\right)$$
$$-\Omega_b\int_{-\infty}^{+\infty} dx\sqrt{1+\tan^2\theta}\{\Delta\breve{g}_{vb}\hat{J}_{vb}\}+\Omega_b\int_{-\infty}^{+\infty} dx\{g'_\sigma\cos(\theta)+g_\sigma\sin\theta\}\frac{\partial}{\partial x}(\sqrt{1+\tan^2\theta}\hat{J}_{vb})-\Omega_b[\{g'_\sigma\cos(\theta)$$
$$+g_\sigma\sin\theta\}\sqrt{1+\tan^2\theta}]_{+\varepsilon}^{-\varepsilon}\hat{J}_{vb}(0)+\{(g_\sigma\cos\theta-g'_\sigma\sin\theta)_{x=+\varepsilon}^{x=-\varepsilon}+g'_g\}\Gamma_\sigma^{-1}J_\sigma(0)+\frac{\Gamma_\sigma^{-1}J_\sigma^2(0)}{2d_a\hat{M}^{trans}}-(g_g)\left(\Omega_b\frac{\partial J_\sigma}{\partial x}\right)_{x=0}$$
$$+\frac{\Gamma_\sigma}{2d_a\hat{M}^{long}}\left(\Omega_b\frac{\partial J_\sigma}{\partial x}\right)_{x=0}^2+\frac{J_\sigma^2(0)}{2\hat{M}^{\pm}}+\int_{-\infty}^{+\infty} dx\sqrt{1+\tan^2\theta}\frac{J_\sigma{}^2}{2\hat{M}_\sigma}+\int_{-\infty}^{+\infty} dx\sqrt{1+\tan^2\theta}\frac{\hat{J}_{vb}{}^2}{2\hat{M}_{vb}}\Bigg]=0. \quad (35)$$

The above expression does not carry any flux and flux gradient discontinuity at the TJ. Therefore, the weak solution method proposed by Ramasubramanian and Shenoy[18] for the symmetrically disposed bicrsytal is valid since $J_\sigma(0)=0$, even though there is a missing term $\{J_\sigma^2(0)/2\hat{M}_\pm\}$ in their formula as we mentioned previously in the development of Eq. (28). The extremum problem represented by Eq. (35) may be solved by some standard methods using the continuous complete sets of functions that satisfy the natural boundary conditions at infinities. The expansion of J_σ and $\hat{J}_{vb}$ by the properly selected complete set of functions involves unknown sets of coefficients, which can be determined via the minimization of the functional by using standard techniques. The best candidate for the asymmetrical problem is the orthonormal Hermite function.[33]

V. NUMERICAL METHODS FOR THE WEAK SOLUTION

In this section, the general outline of the numerical procedure in terms of Hermite functions is provided for the weak solution of thermal grooving problems. We obtained very interesting results from our preliminary computer simulation studies on the nanosized bicrystal interconnect lines ($w_0 \leqslant 100$ nm) having strong anisotropy in the surface specific Gibbs free energy (SSGTE). In order to simplify the mathematical manipulations, the growth (evaporation and condensation) term is completely ignored in this treatment, otherwise our tentative presentation is somewhat cumbersome and bulky.

The surface profile function may be expanded in terms of an orthonormal set of Hermite functions denoted by $\Psi_n(x)$. This function manifold constitutes a well-behaved, complete, and closed set in the infinite interval $-\infty \leqslant x \leqslant +\infty$, and its members vanish with their derivatives very smoothly and extremely fast compared to the Laguerre functions, because the Gaussian function $\exp(-x^2)$ acts as a cofactor (weight function) for the Hermite polynomial $H_n(x)$ in the orthonormality connections. That is, one may write $\Psi_n(x)=\alpha_n H_n(x)\exp(-x^2/2)$, where $\alpha_n=(n!2^n\sqrt{\pi})^{-1/2}$ is the normalization factor. The recursion formulas for Hermite polynomials may be expressible as $H_{n+1}(x)=2xH_n(x)-2nH_{n-1}(x)$ and $dH_n(x)/dx=2nH_{n-1}(x)$. These recursion formulas may be used to derive the following useful connections for the numerical evaluations of Hermite functions and their higher derivatives:

$$\Psi_{n+1}=[\sqrt{2/(n+1)}]x\Psi_n-[\sqrt{n/(n+1)}]\Psi_{n-1},$$

$$\Psi'_n=\sqrt{n/2}\Psi_{n-1}-\sqrt{(n+1)/2}\Psi_{n+1},$$

$$\Psi''_n=\frac{1}{2}[\sqrt{(n+1)(n+2)}\Psi_{n+2}-(2n+1)\Psi_n+\sqrt{(n)(n+1)}\Psi_{n-2}]. \quad (36)$$

The surface profile displacement velocity, which is given by Eq. (12) in terms of the derivative of the surface current density, takes the following form in the absence of the growth term: $\partial y(x,t)/\partial t=-\Omega_b\partial J_\sigma(x,t)/\partial x$. The expansion of both the surface profile and the particle- flux density in terms of the Hermite functions results in $y(x,t)=\Sigma_{n=0}^{n=N}a_n(t)\Psi_n(x)$ and $J_\sigma(x,t)=\Sigma_{n=0}^{n=N}b_n(t)\Psi_n(x)$, respectively. If one substitutes them into the above-mentioned divergence connection, and then applies the orthonormality properties of Hermite functions, the following relationship may be deduced in the presence of the above recursion formulas:

$$\frac{da_n}{dt}=-\Omega_b\sum_{m=0}^{m=N} b_m(t)\langle\Psi_n|\Psi'_m\rangle\cong\Omega_b[b_{n-1}\sqrt{n/2}-b_{n+1}\sqrt{(n+1)/2}]+O(10^{-10}). \quad (37)$$

The antisymmetric transformation matrix $\langle\Psi_n|\Psi'_m\rangle$ between the particle velocity representation and the current field may be given in terms of Kronecker δ functions that is even valid for the matrix elements $n=0$, which cannot be extracted from the above formula explicitly:

$$\langle\Psi_n|\bar{\Psi}'_m\rangle\equiv\langle n|m\rangle'\cong-\sqrt{(m+1)/2}\,\delta_{n,m+1}+\sqrt{m/2}\,\delta_{n,m-1}. \quad (38)$$

This formula contains matrix elements which are exactly represented by the following specific exceptions: $\langle 0|k\rangle' \cong \delta_{1,k}/\sqrt{2}$ and $\langle N|k\rangle' \cong -\delta_{N,k+1}\sqrt{2}$ rows $\langle k|0\rangle' \cong -\delta_{1,k}/\sqrt{2}$ and $\langle k|N\rangle' \cong \delta_{N,k+1}\sqrt{2}$ columns. These matrix elements are approximated in very high precision by better than $O(10^{-10})$, according to the direct numerical evaluations of the associated integrals.

In the normalized and scaled space, one may show the validity of the rigorous relationship $(d/d\bar{t})|\bar{a}_n\rangle = -\Sigma_{m=0}^{m=N}\langle\Psi_n|\bar{\Psi}'_m\rangle|\bar{b}_m\rangle$, as will be proven later in this section. Here, $\bar{b}=\tau_0\ell_0 b$, $\bar{a}=a/\ell_0$, and $\bar{t}=t/\tau_0$. In all these expressions, ℓ_0 is the arbitrary characteristic length and $\tau_0 \equiv \ell_0^4/\Omega_b^2\hat{M}_\sigma g_\sigma^0$ is the previously defined normalized time, which is also used in the strong solution of the problem.[17] In the numerical simulations presented in this work, since the sidewall morphological evolutions are under consideration, we will take $\ell_0=w_0\cong 100$ nm as has been done in the strong solution of the problem. The overbar sign on the symbols indicates the normalized and scaled quantities with respect to the length and time domains. This evolutionary-type ordinary differential equation (ODE) may be integrated using stiffly stable methods[34] to obtain the instantaneous values of the coefficient vector $|\bar{a}\rangle$ of the surface profile in Hermite function space as the basis from the backward information (implicit method) about them.

The main objective as mentioned previously in the present numerical approach is to determine the expansion coefficients of the particle current density from the extremum problem presented formally in Eq. (34). The usual procedure is to substitute the Hermite function expansion of the current density and obtained a function in terms of the expansion coefficients, and then take the variation of that function denoted by $\delta\Xi(b_1,b_2,\ldots,b_N)$ with respect to the free variations of the expansion coefficients presented as $\{\delta b_1,\delta b_2,\ldots,\delta b_N\}$. Then, the next step is to equate all the cofactors of the free variations into zero, which results in a matrix equation having a coefficient matrix of dimension of $(N+1)\times(N+1)$, where $N+1$ is the number of Hermite functions used in the expansion procedure. To simplify the present prototype illustration, the growth terms will be discarded to reduce the size of the procedure, Hence, one may write

$$\delta\Xi\{b_1,\ldots,b_N\} \cong \delta\Bigg(-\Omega_b\sum_n b_n\int_{-\infty}^{+\infty} dx\{g'_\sigma\cos(\theta)+g_\sigma\sin\theta\}\Psi''_n+\Omega_b\sum_n b_n\{(g_\sigma\cos\theta-g'_\sigma\sin\theta)_{x=+\varepsilon}^{x=-\varepsilon}+g'_g\}h_\sigma^{-1}\Psi_n(0)$$
$$-\Omega_b\sum_n b_n[g_g]\Psi'_n(0)+\Omega_b\frac{h_\sigma}{2d_a\hat{M}_{long}}\sum_{n,m} b_nb_m\Psi'_n(0)\Psi'_m(0)+\Omega_b\frac{1}{2d_ah_\sigma\hat{M}_{trans}}\sum_{n,m} b_nb_m\Psi_n(0)\Psi_m(0)$$
$$+\frac{1}{2\hat{M}_\sigma}\sum_{n,m} b_nb_m\int_{-\infty}^{+\infty} dx\sqrt{1+\tan^2\theta}\Psi_n\Psi_m\Bigg)=0. \tag{39}$$

By taking variations of the right side of the above equation with respect to the expansion coefficients, and collecting the terms associated with the arbitrary δb_n variations, one may obtain the following system of linear algebraic equations:

$$-\Omega_b\sum_n \delta b_n\int_{-\infty}^{+\infty} dx\{g'_\sigma\cos(\theta)+g_\sigma\sin\theta\}\Psi''_n+\Omega_b\sum_n \delta b_n\{(g_\sigma\cos\theta-g'_\sigma\sin\theta)_{x=+\varepsilon}^{x=-\varepsilon}+g'_g\}h_\sigma^{-1}\Psi_n(0)-\Omega_b\sum_n \delta b_n[g_g]\Psi'_n(0)$$
$$+\frac{\Omega_b h_\sigma}{2d_a\hat{M}_{long}}\sum_{n,m}[\delta b_nb_m]\Psi'_n(0)\Psi'_m(0)+\left(\frac{\Omega_b}{d_ah_\sigma\hat{M}_{trans}}+\frac{h_\sigma^{-1}}{\hat{M}_\pm}\right)\sum_{n,m}[\delta b_nb_m]\Psi_n(0)\Psi_m(0)$$
$$+\frac{1}{\hat{M}_\sigma}\sum_{n,m}[\delta b_nb_m]\int_{-\infty}^{+\infty} dx\sqrt{1+\tan^2\theta}\Psi_n\Psi_m=0. \tag{40}$$

The solution of the above extremum problem, which constitutes an inhomogeneous set of linear equations, may be represented formally by the matrix notation $\mathbf{A}\cdot\mathbf{b}=\mathbf{c}$. The elements of the scaled and normalized generalized mobility matrix $\mathbf{A}$, which is a symmetric matrix as one expects *a priori*, can be extracted from Eq. (40) and may be given by the expression

$$\mathrm{A}_{m,n}=\frac{\ell_0}{\hat{M}_\sigma}\left[\frac{\bar{\Omega}_b\bar{h}_0\bar{\Psi}'_n(0)\bar{\Psi}'_m(0)}{\bar{d}_a\bar{M}^{long}}+\left(\frac{\bar{\Omega}_b}{\bar{d}_a\bar{h}_\sigma\bar{M}^{trans}}+\frac{1}{\bar{h}_\sigma(\bar{M}_\pm)}\right)\Psi_n(0)\Psi_m(0)+\int_{-\infty}^{+\infty} d\bar{x}\sqrt{1+y_x^2}\Psi_n(\bar{x})\Psi_m(\bar{x})\right]\equiv\frac{\ell_0}{\hat{M}_\sigma}\bar{A}_{m,n}, \tag{41}$$

where the terms between the large square brackets are completely scaled with respect to ℓ_0. Similarly, the mobilities are also normalized with respect to the surface drift-diffusion mobility denoted as $\hat{M}_\sigma=(Dh_\sigma/\Omega_b kT)$, including the mobility $\bar{M}^{\pm}\equiv\ell_0^2\hat{M}^{\pm}/\hat{M}_\sigma$ associated with the corners and edges (i.e., the GB-TJ singularity) of the interfacial layer. By the way, this mobility has identical dimensionality compared to the growth mobility presented previously by $\bar{M}_{vb}=\ell_0^2\hat{M}_{vb}$.[17] The higher dimensionalities in these mobilities are reflected in the $x/\sqrt{t}$ dependence (evaporation condensation) rather than the $x/\sqrt[4]{t}$ or $x/\sqrt[3]{t}$ (the transport by surface diffusion) that is the typical case in the Mullins theory of thermal grooving,[35] which presumes infinite GB-groove tip mobility.

The inhomogeneous part of the linear system, which may be called the capillarity force vector and denoted by $\mathbf{c}$, is represented by the following expression in terms of vector elements:

$$c_n \equiv g_\sigma^0\Omega_b\ell_0^{-1}\Bigg\{\int_{-\infty}^{+\infty} d\bar{x}\{\bar{g}'_\sigma+\bar{g}_\sigma y_x\}/\sqrt{1+y_x^2}\bar{\Psi}''_n(\bar{x}) - \bar{h}_\sigma^{-1}\{(\bar{g}_\sigma\cos\theta-\bar{g}'_\sigma\sin\theta)_{x=+\varepsilon}^{x=-\varepsilon}+\bar{g}'_g\}\Psi_n(0) + [\bar{g}_g]\bar{\Psi}'_n(0)\Bigg\}\equiv g_\sigma^0\Omega_b\ell_0^{-1}\bar{C}_n. \tag{42}$$

The solution of this system of algebraic linear inhomogeneous equations now may be represented by $\mathbf{b}=\mathbf{A}^{-1}\mathbf{c}$, which involves a nonsingular matrix inversion operation only. Then one may combine Eqs. (41) and (42) to obtain the following explicit expression:

$$b_m=[\Omega_b\hat{M}_\sigma g_\sigma^0\ell_0^{-2}]\sum_n \bar{A}_{m,n}^{-1}\bar{C}_n. \tag{43}$$

Hence, by substituting the above finding in Eq. (39) and using the normalization and scaling recipe presented previously, one may deduced the following rigorous relation between the rate of change in surface profile expansion coefficients and the capillary force vector through the generalized mobility matrix denoted by $\bar{A}$:

$$\frac{d\bar{a}_k}{d\bar{t}}=-\frac{\tau_0}{\ell_0}\Omega_b\sum_k b_m\langle k|m'\rangle = -\frac{\tau_0}{\ell_0}[\Omega_b^2\hat{M}_\sigma g_\sigma^0\ell_0^{-3}]\sum_{m,n}\langle k|\bar{m}\rangle'\bar{A}_{m,n}^{-1}\bar{C}_n = -\sum_{m,n}\langle k|\bar{m}\rangle'\bar{A}_{m,n}^{-1}\bar{C}_n,$$

$$\dot{\bar{a}}=-\bar{T}\bar{A}^{-1}\bar{C}, \tag{44}$$

where $\bar{T}_{k,m}\equiv\langle k|\bar{m}\rangle'$ is the scaled transformation matrix, which is advocated by the author in a precise format, and it is introduced explicitly in Eq. (38). In the case of a very high tolerance index ($\leqslant 10^{-32}$) the above-mentioned specific rows and columns should be numerically evaluated. The time integration of the stiff ODE denoted by Eq. (44) can be now easily performed by using one of the stiff stable methods. After trying all possible orders, which are in the range of $k\leqslant 6$ by employing the formulas presented in the literature after the celebrated work of Gear,[34] we have found that the second-order[36] works best for the present stiff ODE system. The main difficulties in the computer simulations using variational approach arise in the numerical integration of the capillary integrand presented by the first term in $\bar{C}$, and its conjugated part given by the last term in the generalized mobility $\bar{A}$. In particular, the first integral is very troublesome when the higher-order Hermite functions ($n\geqslant 30$) are involved in the case of strong anisotropy. The situation becomes even worse if one tries to represent the cusped regions in the Wullf construction of the Gibbs surface free energy by a function having abrupt change in the slope (discontinuity in the first derivative). We have surmounted this difficulty by dividing the integration domain into subsegments determined by the roots of the integrand, and then applying the Gauss-Legendre quadrature formula using up to 60-point abscissas and weights for each subdomain, and summing them up to get the final answer in any degree of precision. This modification resulted in a very powerful integrator compared to those standard integrators available in the literature, in terms of error accumulation and computational speed, as long as one stays in the same tolerance precision index level.

In Eq. (42), the expression denoted by $\bar{g}_\sigma\equiv\bar{g}_\sigma(\hat{\theta},\hat{\phi};m)$ is the angular part of the anisotropic surface specific Gibbs free energy, and g_σ^0 corresponds to the minima in the Wullf construction of surface free-energy topography. By following the general trend, one may introduce the trigonometric representation by defining the tilt angle $\hat{\phi}$ as such that the surface normal of a selected vicinal plane coincides with the x axis when $\hat{\phi}=0$. Hence, one writes the angular part of the expression for anisotropic surface Gibbs free energy, where $\hat{\theta}=\pi/2-\theta$ is the angle between the line normal vector of the diffusion plane of a generalized cylindrical surface projected into 2D space and the x axis of the global Cartesian reference system as

$$\bar{g}_\sigma(\hat{\theta},\hat{\phi};m)=\{1+B\sin^2[m(\hat{\theta}-\hat{\phi})]\}. \tag{45}$$

Here, $\hat{m}=2m$ corresponds to the $2\pi/\hat{m}$ degree of rotational folding associated with the zone axis of a given family of planes over which diffusion takes place during the morphological evolution of the edges or the sidewalls of thin single-crystal films. $B\geqslant 0$ is the surface specific Gibbs free-energy anisotropy constant, which is a positive quantity in the above *ad hoc* representation, and measures fractional degrees of roughness on the Wulff construction of the specific surface Gibbs free energy. One may show that for the existence of the absolute stability regimes,[37] where the surface stiffness should stay as a positive definite quantity in all conceivable orientations, the following set of upper limits (threshold levels) for the anisotropy constants must be obeyed: $B\leqslant\{1,1/7,1/17\}$ in the case of two-, four-, and sixfold symmetries, respectively.

In the numerical work, one may use the following very good but tentative approximations: $\bar{d}_a\cong\bar{h}_\sigma$ and $\bar{\Omega}_b\cong d_a^3$. Here, $\bar{h}_\sigma=h_\sigma/w_\sigma$, the normalized thickness of the interfacial

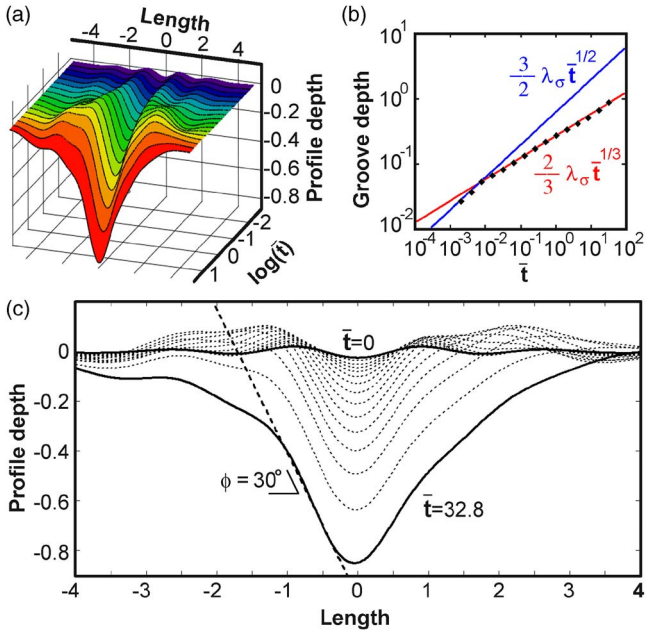

FIG. 2. (Color online) The morphological evolution of a grain-boundary groove subjected to anisotropic surface specific Gibbs free energy (the surface stiffness). Both grains have identical textures with fourfold rotational symmetries characterized by the (001) top surface having the [100] direction oriented with $\hat{\phi}=30°$ tilt angle. Anisotropy level $B=0.1<1/7$, $\bar{M}^{long}=1$, $\bar{M}^{trans}=0.001$, $M^{\pm}=0.001$, $h_\sigma=0.1$, and $\lambda_\sigma=0.6$. (a) 3D groove evolution during the first $\bar{t}=30$. (b) Groove depth versus time plot that indicates initial $\sqrt{\bar{t}}$ dependence and then switches to $\sqrt[3]{\bar{t}}$ behavior on a double-logarithmic scale. (c) Facet formation with an angle $\hat{\phi}=30°$ at the groove wall on the left side ($x<0$).

layer with respect to the specimen width (or thickness) should be supplied as an input parameter to the numerical simulations, and its value definitely depends upon the actual size of the interconnect specimen, namely, the width or the thickness. The most accepted value of the interfacial layer (a few monolayers) is roughly on the order of a few atomic distances. Therefore, for a nanosized interconnect line ($w_0 \leqslant 30-50$ nm) to be used in ultralarge-scale integrated circuits for microelectronic applications, one has $h_\sigma \approx 0.01$. There are three more additional input parameters $\{\bar{M}^{long}, \bar{M}^{trans}, \bar{M}^{\pm}\}$ to complete the parametric set required for the numerical simulations, and they are, respectively, associated with normalized mobilities related to the GB-groove tip displacement, the transverse current flow across the GB TJ, and the mobility due to the abrupt variation of the capillary chemical potential at the junction. Therefore, one has to work in the four-dimensional parametric space for the computer simulation experiments.

In Fig. 2(a), the results of our tentative computer simulation studies on the morphological evolution associated with GB thermal grooving of the sidewall surfaces of an interconnect bicrystal line having face-centered-cubic (fcc) structure are presented in a 3D plot. To reveal the kinetics of the groove tip displacement, the normalized groove depth is plotted with respect to the normalized time on a double-logarithmic scale as shown in Fig. 2(b). This figure clearly illustrates two stages of the power-law time dependence, and its conversion at the sharp knee point at $\bar{t}=0.01$, where the time dependence changes abruptly from $\sqrt{\bar{t}}$ dependence to $\sqrt[3]{\bar{t}}$ behavior for the system parameters used in this experiment. In these simulations, only the first 15 orders of Hermite functions are used in the expansion procedure, which resulted in a reasonably good reproduction of the surface profile, since the anisotropy constant $B=0.1\leqslant 1/7$ is so chosen that no Dirac δ function singularity occurs in the surface stiffness function at the vicinal planes. The slope variation on the surface profile in the vicinity of the GB groove shows that the groove wall on the left side ($x<0$) of the GB TJ has a tendency for the formation of a soft faceting close to the take-off angle about 30° [Fig. 2(c)], which is in a good agreement with the chosen tilt angle $\hat{\phi}=30°$ for the present simulation work. Since the function used in the description of the anisotropy does not have a discontinuity similar to the one employed by Ramasubramaniam and Shenoy,[18] no sharp faceting can be expected in the present work. Here, one should recall that originally flat sidewall surfaces of the bicrystal interconnect line correspond to the vicinal $(0\bar{1}0)$ planes in the case of zero tilt angle. This study gives two universal analytical expressions which are given in the normalized space, and they contain the wetting parameter λ_σ explicitly, namely, $\bar{H}_{depth}=(3\lambda_\sigma/2)\sqrt{\bar{t}}$ and $(2\lambda_\sigma/3)\sqrt[3]{\bar{t}}$ for the initial and final stages of the evolution process. The wetting parameter may be given by $\lambda_\sigma=g_g/2g_\sigma^0$, where g_g and g_σ^0 are the specific surface Gibbs free-energy densities associated, respectively, with the grain boundary and the void surface layers, and defined previously.

This experiment has shown that the groove depth displacement kinetics does not depend very much on the longitudinal mobility in the range of $\bar{M}_{long}=0.1-10$, and it does not follow Mullins' isotropic one-fourth power law[3] for the normalized run times used in these experiments because of the extremely high anisotropy constant selected for the SSGFE, which is just below the instability threshold level above which the surface stiffness becomes negative. However, Ramasubramaniam and Shenoy in their simulation studies have recovered this expected scaling power law for their large junction mobilities $\tilde{M}\cong 100-1000$. Here one should remark that the following connection exists between their normalized mobility denoted by $\tilde{M}$ [Eq. (15) in Ref. 18] and the normalized longitudinal mobility defined in this paper, namely, $\tilde{M}\cong\bar{\Omega}_b^{-1}\bar{M}_{long}\cong\bar{h}_\sigma^{-3}\bar{M}_{long}$, which clearly indicates that there are many orders of magnitude difference between these quantities, depending upon the length scale ℓ_0 used in the simulations. Unfortunately, the above-cited authors in their remarkably thorough paper have used the geometric representation (i.e., the flux in dimensions of $J_\sigma[l^2/t]$, and the surface drift diffusion mobility as $D[l^6/\text{energy}\times t]$), and did not employ the physicochemical quantities to describe the kinetics of surface diffusion as well as the capillary chemical potential in the conventional particle representation introduced by Herrings[1] and Mullins.[3] That makes it very difficult to compare our results with theirs on a quantitative basis especially in the normalized time domain. In the

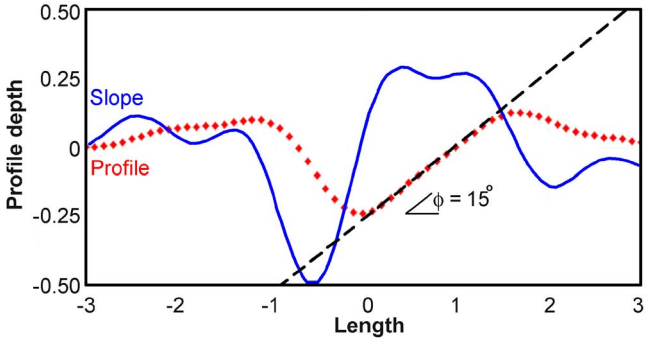

FIG. 3. (Color online) Steady-state profile of the faceted groove obtained by using a trigonometric function for the anisotropic SSGFE, which describes cusp formations in the Wulff construction at $\phi+n\pi/2$, $n=0,1,2,\ldots$, having fourfold rotational symmetry, where the tilt angle $\phi R=15°$, $\lambda_\sigma=0.6$, and the anisotropy constant $c=0.4$ are utilized. Input data: $\bar{M}^{long}=1.0$, $\bar{M}^{trans}=0.001$, $\bar{M}^{\pm}=0.001$, and $h_\sigma=0.01$.

present simulation study, both grains are assumed to have exactly the same textures, and the top surface of the line coincides with the $(001)\times[100]$ crystal plane of a face-centered-cubic crystal.

In Fig. 3, the steady-state profile of a faceted groove is presented, where the fourfold symmetry in the surface specific Gibbs free-energy anisotropy is described by the formula used successfully by Ramasubramaniam and Shenoy[18] to study symmetrical groove profiles, namely, $\bar{g}_\sigma=[1-c+c\{|\sin(\theta-\phi)|+|\cos(\theta-\phi)|\}]$. Here c is the anisotropy constant bounded by $0\leqslant c\leqslant 1$, This function shows cusps that are seen at the facets orientations $\phi+n\pi/2$, $n=0,1,2,\ldots$, and can be shown to have origins in the energetics of crystallographic surface steps.[38] The windward side $(x>0)$ of the above figure is in excellent agreement with the result reported by Ramasubramaniam and Shenoy (Fig. 8b in Ref. 18) using the exactly same physicochemical parameters for their symmetrically disposed bicrystal specimens, where they employed 30 Laguerre functions as basis in connection with the standard Laguerre-Gauss-Radau quadrature software compared to our usage of the modest number of 15 Hermite functions in a standard FORTRAN run in a PC environment, utilizing a completely home-designed integrator.

In Fig. 4 the results of a computer simulation carried out on a fcc bicrystal metallic interconnect line having 300 nm width ($\bar{h}_\sigma=0.001$), and a special microstructure (texture) associated with the (100) top surface are presented. In this simulation, the grains on the left and right sides of the GB are oriented, respectively, at $\phi L=165°$ and $\phi R=45°$ tilt angles with respect to the longitudinal x axis of the interconnect line. The high GB-TJ displacement mobility $\bar{M}_{long}=100$ combined with the high transverse mobility $\bar{M}^{trans}=100$ have resulted in a conversion in the power-law exponent first from $\sqrt{\bar{t}}$ to $\sqrt[3]{\bar{t}}$ and then from $\sqrt[3]{\bar{t}}$ to $\sqrt[4]{\bar{t}}$ dependence at the normalized time given by the sharp knees on the log-log plot represented by $\bar{t}_{knee}=0.01$ and 1, respectively. This experiment definitely illustrates that for the longer annealing times combined with the high transverse current mobility, the

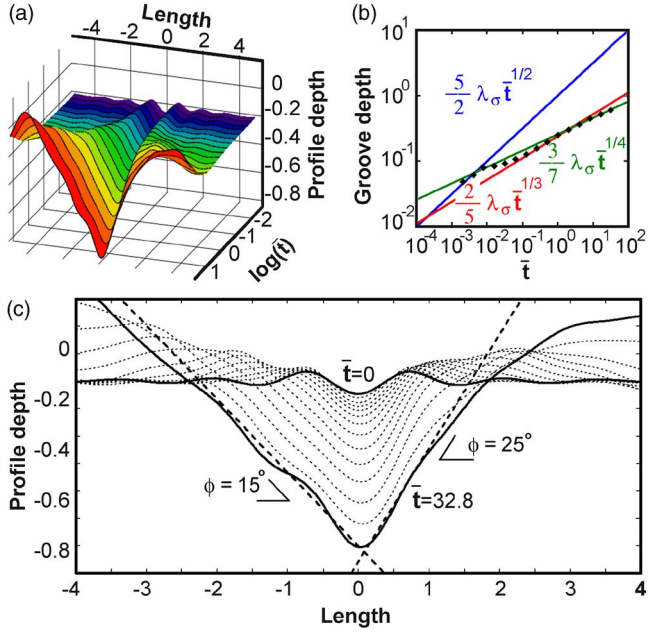

FIG. 4. (Color online) Quasistationary surface profile of the faceted groove and the associated GB-TJ displacement plot are obtained by using a trigonometric function for the anisotropic SSGFE, which describes cusp formations in the Wulff construction at $\phi+n\pi/2$, $n=0,1,2,\ldots$, where $\phi L=165°$ and $\phi R=45°$, $\lambda_\sigma=0.6$, and the anisotropy constant $c=0.4$ are utilized. Input data: $\bar{M}^{long}=100$, $\bar{M}^{trans}=100$, $\bar{M}^{\pm}=0.001$, and $\bar{h}_\sigma=0.001$. Time step is $\Delta\bar{t}=0.002$. (a) 3D groove evolution during the first $\bar{t}=30$. (b) Groove depth versus time plot that indicates initial $\sqrt{\bar{t}}$ dependence then first switches to $\sqrt[3]{\bar{t}}$ followed by another transition to $\sqrt[4]{\bar{t}}$ behavior on a double-logarithmic scale. (c) Facet formation with an angle $\hat{\phi}=165°$ at the groove wall on the left side $(x<0)$.

grain-boundary kinetics recovers its isotropic power-law exponent as first derived by Mullins in his analytic treatment of the isotropic case. The left side reaches the faceting angle $\phi L=165°$ very rapidly, in contrast to the right side, which is being trapped at the smooth face with an inclination of $\phi R\cong 25°$ instead of a 45° facet angle. On the other hand the simulation experiment done on the sample having a grain texture represented by the tilt angles $\phi R\cong 15°$ and $\phi L=150°$ showed almost excellent faceting at both faces of the grain-boundary groove showing, respectively, exactly the same facet angles, where $\bar{M}_{long}=1$ and $\bar{M}_{trans}=1$ are used in connection with $\bar{h}_\sigma=0.1$. The grooving kinetics for this experiment are found to be describable by the power law represented by $\sqrt[3]{\bar{t}}$ without showing any knee on the log-log plot.

This unusual trapping phenomenon does not change if one reflects the grain texture with respect to the GB, and/or uses different sets of mobility parameters. This anomalous situation shows that at high tilt angles close to 45° and 90° for the fourfold rotational symmetry, the equilibrium configuration at the groove tip cannot be reached fully over the entire duration of the simulation. This point should be further check using much higher-order Hermite functions in the expansion combined with very short time steps using increased run time to see whether it is a numerical artifact or a physical reality.

Similar trapping nonequilibrium behavior is also observed in Ramasubramaniam and Shenoy's experiments in a completely different context.

VI. DISCUSSION AND CONCLUSIONS

As we mentioned in the Introduction of this paper the majority of the work on surfaces and interfaces relies on the equilibrium configuration of the TJ singularity due to the lack of a theoretical treatment of nonequilibrium problems related to solid state surfaces and interfaces. There are a few exceptions such as the celebrated work of Bedeaux and co-workers[39–41] and the studies of Shikhmurzaev.[42,43] These authors a the hydrodynamic approach applied to the Gibbs geometric interface model, with completely different objectives and context. Recently, an irreversible thermodynamic treatment of solid surfaces and interfaces with TJ singularities in 2D and 3D anisotropic media was formulated by the present author by further advocating the discrete microfinite-element method[17] in connection with local and the global internal entropy production associated with the displacement of simply or multiply connected interfacial layers.[30] The first serious attempt to obtain a weak solution of the extremum problem associated with surfaces with symmetrically disposed GB TJs by the variational method has been made by Ramasubramanian and Shenoy;[18] it relies on the Herring treatment of the surfaces based on equilibrium thermodynamics and *ad hoc* thermokinetics connections. Therefore, in principle their approach is nothing to do with the irreversible thermodynamics treatment advocated in this paper to get the strong as well as the weak solution of the problem.

The various continuity conditions imposed on the GB-TJ current density are not as trivial as suggested by Ramasubramaniam and Shenoy,[18] by relying on the conclusion that the $\partial h/\partial t$ continuity of the surface displacement rate is sufficient for the continuity of the gradient surface flux density. First of all, the surface flux density as defined by Herring's formula and used in their formulation gives a Dirac δ function singularity at the GB TJ, and its derivative $\delta'(x)$ definitely gives a generalized function for the gradient of the current density and may be given in terms of a point-source function basis, $\delta'(x) \Leftarrow \lim_{\varepsilon\to 0}\{-(2x/\varepsilon^3\sqrt{\pi})\exp(-x^2/\varepsilon^2)\}$, which shows plus/minus infinite oscillation at the origin. It has operational meaning only in the integral representation $\int dx\, J(x)\delta'(x) \Rightarrow J'(0)$, as can be proved very easily. This seemingly awkward mathematical dilemma comes from the improper usage of equations such as Eq. (11) derived for the ordinary points along sufficiently smooth curves or surfaces, and applied directly to the singularities such as corners, edges, and finally free-moving cusps such as GB TJs. In this paper we have also proved as a by-product of the variational GIEP formalism that at corners the Herring formula given by Eq. (14), which states that the current density is proportional to the gradient of the surface chemical potential does not apply, but rather the surface flux density becomes a function of surface chemical potential difference, given by Eq. (19). One can easily design a simple gedanken experiment to prove the validity of the above statements as proposed by the author and fully quoted by Averbuch *et al.*[9] in their analytical paper on the subject of GB grooving under capillary and EM forces.

The weak solution of the problem is formulated as an extremum problem referring to the strong solution obtained by the nonequilibrium thermodynamic formalism as a mathematical basis in terms of particle current density representation. The success of the weak solution of any problem in engineering sciences is closely associated with its adaptability to the well-known numerical methods that use one of the class of complete and closed orthonormal functions satisfying the boundary conditions of the physical problem at some points, especially at infinities. Therefore, the extremum problem should be cast in such a manner that the surface current density and its first derivatives, which appear in the formulation, should be continuous functions everywhere including the GB-TJ singularity. This objective is accomplished in this paper by using a simple mathematical technique in collaboration with the feedback obtained from the DMFE method to smooth out the discontinuities in the surface particle-flux density and its derivatives at the GB TJ.

The procedure adopted allows us to handle the weak solution in the function space characterized by $C_1(-\infty,+\infty)$, and introduces an extreme simplification in the numerical methods by permitting us to use Hermite orthonormal functions in the morphological evolution of surfaces with asymmetric GB voiding that are exposed to anisotropic surface stiffness. In Sec. V, the numerical method for the weak solution of the extremum problem is fully elaborated in a completely normalized and scaled parametric space in terms of a rather compact matrix representation. The various critical but tentative applications of the weak solution are demonstrated and compared with the available literature, and found excellent agreement with the special cases elaborated by Ramasubramaniam and Shenoy,[18] who have done pioneering work in this field.

The present author, who has advocated both methods dealing with the irreversible thermodynamics of solid surfaces and interfaces, believes that both formalisms may have their own merits in the solutions of practical problems. The DMFE method has profound flexibility in using the strong solution in computer simulations of various practical problems having complicated boundary conditions, compared to the variational formulation, which primarily employs the weak solution of the problem in terms of a set of orthonormal functions that satisfies the boundary conditions at least at infinity. Furthermore, the DMFE method can be easily programmed for PC applications, even for the MATHCAD environment. The variational formulation of the weak solutions proposed in this paper may be easily extended for the 3D space, as has been done recently for the discrete microelement method,[30] Then, it may be used in the treatment of 3D systems having complicated specimen geometries by novel programming techniques such that commercially available finite element and/or boundary element method subroutines could be used for mainframe computations. The main numerical problem encountered by the author dealing with the weak solution of the variational asymmetric problems is the lack of any standard integrator in the literature to handle the

integrand associated with the capillarity term, which shows unusual oscillations and discontinuities especially in the vicinity of the Dirac δ function singularity at the cusp regions if one has to use high-order Hermite functions as basis. That is just opposite to the symmetrical case, where Laguerre functions can be used as was done by Ramasubramanian and Shenoy,[18] and there is highly sophisticated software available in the literature dealing with spectral elements theory in mathematical physics. However, our group have succeeded in developing our tailor-made integrator by closely inspecting the behavior of the integrand function using the graphical and computational facilities of MATCAD-13, and modifying the Gauss-Legendre integrator accordingly.

ACKNOWLEDGMENTS

The author wishes to thank Dick Bedeaux of Norwegian University of Science and Technology, Trondheim for his very valuable comments and motivation concerning our approach to the irreversible thermodynamics of solid surfaces and interfaces in the present context. The author also thanks his former student and co-worker Ersin Emre Oren of University of Washington, Seattle, for his valuable and constant interest in the development of the software for the integrator, and Oncu Akyildiz for the mainframe computer programming. This work is partially supported by the Turkish Scientific and Technical Research Council TUBITAK Grant No. 104M399.

*FAX: +90 312 210-1267. Email address: ogurtani@metu.edu.tr; url: http://www.csl.mete.metu.edu.tr

[1] C. Herring, in *The Physics of Powder Metallurgy*, edited by W. E. Kinston (McGraw-Hill, New York, 1951), p. 143.
[2] J. von-Neumann, *Metal Interfaces* (ASM, Cleveland, 1952), p. 108.
[3] W. W. Mullins, J. Appl. Phys. **28**, 333 (1957).
[4] W. Gibbs, *The Collected Works of J. Willard Gibbs, Vol. I: Thermodynamics* (Yale University Press, New Haven, CT, 1948), p. 226.
[5] T. Young, Philos. Trans. R. Soc. London **95**, 65 (1805).
[6] M. Mahadevan and R. M. Bradley, Physica D **126**, 201 (1999).
[7] A. Kazaryan, Y. Wang, and B. R. Patton, Scr. Mater. **41**, 487 (1999).
[8] J. W. Cahn, C. Elliott, and A. Novick-Cohen, Eur. J. Appl. Math. **7**, 287 (1996).
[9] A. Averbuch, M. Israeli, M. Nathan, and I. Ravve, J. Comput. Phys. **188**, 640 (2003).
[10] E. Rabkin, L. Klinger, and V. Semenov, Acta Mater. **48**, 1533 (2000).
[11] L. Klinger and E. Rabkin, Interface Sci. **9**, 55 (2001).
[12] W. Zhang, P. Sachenko, and I. Gladwell, Acta Mater. **107**, 16 (2004).
[13] T. Xin and H. Wong, Acta Mater. **51**, 2305 (2003).
[14] T. O. Ogurtani and O. Akyildiz, J. Appl. Phys. **97**, 093520 (2005).
[15] E. E. Oren and T. O. Ogurtani, in *Thin Films: Stresses and Mechanical Properties IX*, edited by C. S. Ozkan, R. C. Cammarata, L. B. Freund, H. Gao, MRS Symposia Proceedings No. 695 (Materials Research Society, Pittsburgh, 2002), p. L.5.5.1.
[16] T. O. Ogurtani and E. E. Oren, J. Appl. Phys. **97**, 7246 (2004).
[17] T. O. Ogurtani and E. E. Oren, Int. J. Solids Struct. **42**, 3918 (2005).
[18] A. Ramasubramaniam and V. B. Shenoy, Acta Mater. **53**, 2943 (2005).
[19] Z. Suo, Adv. Appl. Mech. **33**, 193 (1997).
[20] T. O. Ogurtani and E. E. Oren, J. Appl. Phys. **90**, 1564 (2001).
[21] J. E. Verschaffelt, Bull. Cl. Sci., Acad. R. Belg. **22**, 373 (1936).
[22] E. A. Guggenheim, *Thermodynamics*, 3rd ed. (North-Holland, Amsterdam, 1959), p. 46.
[23] D. Bedeaux, Adv. Chem. Phys. **64**, 47 (1986).
[24] A. D. Myskis, *Advanced Mathematics for Engineers* (MIR, Moscow, 1975), p. 357.
[25] F. B. Hildebrand, *Methods of Applied Mathematics* (Prentice-Hall, Englewood Cliffs, NJ, 1961), p. 127.
[26] R. Haase, *Thermodynamics of Irreversible Processes* (Addison-Wesley, Reading, MA, 1969), p. 245.
[27] T. O. Ogurtani and A. K. Seeger, J. Chem. Phys. **79**, 5041 (1983).
[28] S. R. De Groot, *Thermodynamics of Irreversible Processes* (North-Holland, Amsterdam, 1961), p. 59.
[29] L. Onsager, Phys. Rev. **37**, 405 (1931); **38**, 2265 (1931).
[30] T. O. Ogurtani, J. Chem. Phys. **124**, 144706 (2006).
[31] J. M. Blakely, *Properties of Crystal Surfaces* (Pergamon Press, Oxford, 1973), p. 19.
[32] A. Needleman and J. R. Rice, Acta Metall. **28**, 1315 (1980).
[33] L. F. Lösch and J. E. Lösch, *Tables of Higher Functions* (McGraw-Hill, New York, 1960) p. 101.
[34] C. W. Gear, *Numerical Initial Value Problems in Ordinary Differential Equations* (Prentice-Hall, Englewood Cliffs, NJ, 1971), p. 109.
[35] W. W. Mullins, J. Appl. Phys. **28**, 333 (1957).
[36] G. Dahlquist, Proc. Symp. Appl. Math. **15**, 147 (1963); BIT, Nord. Tidskr. Inf.behandl. **3**, 27 (1963).
[37] T. O. Ogurtani (unpublished).
[38] P. Nozieres, in *Solids far from Equilibrium*, edited by C. Godreche (Cambridge Univeristy Press, Cambridge, U.K., 1992), pp. 1–154.
[39] D. Bedeaux, Adv. Chem. Phys. **64**, 47 (1986).
[40] D. Bedeaux, J. Chem. Phys. **120**, 3744 (2004).
[41] D. Bedeaux, S. Kjeistrup, and J. M. Rubi, J. Chem. Phys. **119**, 9163 (2003).
[42] Y. D. Shikhmurzaev, J. Fluid Mech. **334**, 211 (1997).
[43] Y. D. Shikhmurzaev, Int. J. Multiphase Flow **19**, 598 (1993).